MUSCULAR & MECHANICAL EFFICIENCY IN CYCLING

by

Oliver Blake
B.Sc., University of Guelph, 2002

THESIS SUBMITTED IN PARTIAL FULFILLMENT OF
THE REQUIREMENTS FOR THE DEGREE OF

MASTER OF SCIENCE

In the
Department of Biomedical Physiology and Kinesiology
of
Faculty of Science

© Oliver Blake, 2011

SIMON FRASER UNIVERSITY

Summer 2011

APPROVAL

Name: **Oliver Blake**

Degree: **Master of Science**

Title of Thesis: **Muscular & Mechanical Efficiency in Cycling**

Examining Committee:

             Chair: **Dr. Tom Claydon**
Assistant Professor of Department of Biomedical
Physiology and Kinesiology

_____

Dr. James Wakeling
Senior Supervisor
Assistant Professor of Department of Biomedical
Physiology and Kinesiology

_____

Dr. Max Donelan
Supervisor
Associate Professor of Department of Biomedical
Physiology and Kinesiology

_____

Dr. David Sanderson
External Examiner
Senior Associate Director of the School of Human
Kinetics
University of British Columbia

Date Defended/Approved: June 14, 2011

Declaration of Partial Copyright Licence

The author, whose copyright is declared on the title page of this work, has granted to Simon Fraser University the right to lend this thesis, project or extended essay to users of the Simon Fraser University Library, and to make partial or single copies only for such users or in response to a request from the library of any other university, or other educational institution, on its own behalf or for one of its users.

The author has further granted permission to Simon Fraser University to keep or make a digital copy for use in its circulating collection (currently available to the public at the "Institutional Repository" link of the SFU Library website <www.lib.sfu.ca> at: <http://ir.lib.sfu.ca/handle/1892/112>) and, without changing the content, to translate the thesis/project or extended essays, if technically possible, to any medium or format for the purpose of preservation of the digital work.

The author has further agreed that permission for multiple copying of this work for scholarly purposes may be granted by either the author or the Dean of Graduate Studies.

It is understood that copying or publication of this work for financial gain shall not be allowed without the author's written permission.

Permission for public performance, or limited permission for private scholarly use, of any multimedia materials forming part of this work, may have been granted by the author. This information may be found on the separately catalogued multimedia material and in the signed Partial Copyright Licence.

While licensing SFU to permit the above uses, the author retains copyright in the thesis, project or extended essays, including the right to change the work for subsequent purposes, including editing and publishing the work in whole or in part, and licensing other parties, as the author may desire.

The original Partial Copyright Licence attesting to these terms, and signed by this author, may be found in the original bound copy of this work, retained in the Simon Fraser University Archive.

Simon Fraser University Library
Burnaby, BC, Canada

STATEMENT OF
ETHICS APPROVAL

The author, whose name appears on the title page of this work, has obtained, for the research described in this work, either:

(a) Human research ethics approval from the Simon Fraser University Office of Research Ethics,

or

(b) Advance approval of the animal care protocol from the University Animal Care Committee of Simon Fraser University;

or has conducted the research

(c) as a co-investigator, collaborator or research assistant in a research project approved in advance,

or

(d) as a member of a course approved in advance for minimal risk human research, by the Office of Research Ethics.

A copy of the approval letter has been filed at the Theses Office of the University Library at the time of submission of this thesis or project.

The original application for approval and letter of approval are filed with the relevant offices. Inquiries may be directed to those authorities.

Simon Fraser University Library
Simon Fraser University
Burnaby, BC, Canada

ABSTRACT

In cycling some muscle coordination patterns result in high power outputs whereas others are more efficient. This study examined mechanical factors that affect muscle activity to identify coordination patterns used for different power outputs, total muscle activation and muscle activation effectiveness to produce power in cycling.

Electromyography, pedal forces, kinematics, power output, cadence and slope were measured and compared indoors and/or outdoors in competitive cyclists at a range of resistances indoors and natural resistances during a time-trial outdoors.

A trade-off existed between high power and high overall mechanical efficiency. Increased efficiency was dependent on the coordination of all muscles and independent of pedal force direction, while high power resulted from elevated activity of only a few muscles. Muscle coordination was influenced by workload and slope through altered power output or cadence. The study highlights the importance of specificity in cycling training to maximize exposure to competition specific muscle coordination patterns.

Keywords: Electromyography; Power Output; Pedal Forces; Kinematics; Time Trial; Slope

ACKNOWLEDGEMENTS

TABLE OF CONTENTS

LIST OF FIGURES

CHAPTER 1: INTRODUCTION

Cycling is a repetitive activity utilizing coordinated combinations of leg muscles to apply force to the pedals. The muscle activity and coordination can vary dramatically between people throughout a single pedal cycle and between different pedal cycles of the same person (Hug et al., 2004; Jammes et al., 2001). Even amongst elite cyclists where training backgrounds and physical attributes are similar there is variation in the muscle coordination patterns used to complete a pedal cycle (Hug et al., 2004). It is important to address muscle performance and behavior in both indoor and outdoor cycling due to possible discrepancies. Environmental conditions in outdoor cycling, such as the slope, influence both the cadence and power output in male cycling competitions. Cyclists use lower cadences (Lucia et al., 2001) and higher power outputs in mountainous versus flat stages (Padilla et al., 2001; Vogt et al., 2006) of male multi-stage cycling races. They also have higher mean power outputs in time trials versus group stages (Mujika & Padilla, 2001). It is necessary to consider the environmental influences on cadence and workload because both cadence and workload affect muscle coordination (Hug & Dorel, 2009; Wakeling & Horn, 2009). The amount of muscle activity reflects the metabolic costs of cycling (Arnaud et al., 1997; Bigland-Ritchie & Woods, 1976) and muscle efficiency is the ratio of mechanical work to the total metabolic costs to produce the work (Whipp & Wasserman, 1969). Therefore, comparisons of muscle timing, coordination and activity levels to factors affecting mechanical work, such as cadence, pedal forces, kinematics and terrain may provide valuable insight into cycling efficiency and performance.

1.1 Muscle Timing & Coordination

Given that cycling is a constrained movement, the timing of muscle activation is typically referenced to 360° of a pedal cycle. Some studies use onset and offset times based on a predetermined threshold to identify muscle activation timing, though this method does not provide information about the shape of the activity envelope. Others compare the root mean square profile of different pedal cycles using a coefficient of

cross correlation, which provides more information about the timing relative to the pedal cycle. The muscle coordination patterns of a pedal cycle have been described with varying results and are dependent on the cycling background of the subjects, pedals and shoes, load, cadence, fatigue and body position (see review (Hug & Dorel, 2009)).

The timing and coordination of muscle activation plays a significant role in the amount of muscle activity used during a pedal cycle. For example longer durations of activation and more muscle co-contraction contribute to increased muscle activity. During sustained sub-maximal running, different leg muscle coordination patterns have been identified for similar running styles (Wakeling et al., 2001). One explanation was that the compensation of agonistic muscles resulted in similar muscle force patterns with differing recruitment patterns (Wakeling et al., 2001). In elite cyclists there is considerable variation between subjects during incremental exercise to exhaustion for vastus lateralis (VL), vastus medialis (VM), gluteus maximus (GM), rectus femoris (RF), semimembranosis, biceps femoris (BF), lateral gastrocnemius (LG), and tibialis anterior (TA) activity (Hug et al., 2004). GM, VL and VM have the lowest variation in the timing of activation when calculated at 10% intervals of the pedal cycle (Ryan & Gregor, 1992). It has been suggested that the low levels of variation in these muscles provides support for their roles as primary power producers in cycling (Ryan & Gregor, 1992). In contrast the RF, BF and semitendinosus (ST) exhibit high levels of variability. Regardless of the leg muscle, the variability is highest in the first 20% of the pedal cycle (Ryan & Gregor, 1992). These studies highlight the enormous variation in muscle activity through altered coordination despite the controlled cyclical motion of cycling.

Cycling cadence also affects the timing of muscle activation relative to a pedal cycle (Neptune et al., 1997; Sarre & Lepers, 2005). Increased cadence results in earlier activation of RF, BF (Neptune et al., 1997; Sarre & Lepers, 2005), TA, GM (Li, 2004; Neptune et al., 1997), VL (Li, 2004; Sarre & Lepers, 2005), medial gastrocnemius (MG), VM, SM (Neptune et al., 1997) and LG (Sarre & Lepers, 2005). It has been suggested that this is to overcome the electromechanical delay, which is the delay in time between the onset of electromyography (EMG) and the application of force, to apply torque to the crank arm at a consistent position within each pedal cycle, despite the cadence (Neptune et al., 1997; Sarre & Lepers, 2005).

1.2 Quantity of Muscle Activity

Along with timing, the amplitude of leg muscle activity has a major impact on energy consumption and cycling efficiency. Increases in muscle activity may or may not be beneficial to cycling efficiency depending upon which muscles are active, the amount of activity and the timing and duration of activation relative to the pedal cycle. For example trained cyclists prefer high cadences that minimize neuromuscular fatigue regardless of the elevated metabolic cost (Sarre & Lepers, 2005; Takaishi et al., 1996). Also potentially confusing the cycling efficiency equation is co-contraction of agonist/ antagonist muscle pairs that occur in cycling (van Ingen Schenau et al., 1992). It has been suggested that this strategy stabilizes the joints for energy transfer reducing muscle stress and mechanical energy expenditure (Hug & Dorel, 2009; van Ingen Schenau et al., 1992).

The primary muscles involved in cycling power production are the VL and VM (Bini et al., 2008; Ryan & Gregor, 1992). They display the highest peak activity levels (approximately 50% and 85% of their maximum voluntary contraction for 120 W and 240 W respectively) relative to the maximum voluntary contraction, while GM and RF show the lowest peak activity levels (less than 12% and 40% for 120 W and 240 W respectively) (Ericson et al., 1985). Activation levels between different subjects vary considerably, yet within the same subject the activity level is consistent for different trials (Dorel et al., 2008). In comparison to highly trained cyclists, novice cyclists show less variation in the amplitude of muscle activity in the muscles of the lower leg (TA, LG and soleus (Sol)) (Chapman et al., 2008). These discrepancies between different subjects and cycling experience helps explain differences in the quantity of muscle activity, but does not clarify how changes in workload affect the muscle activity nor how this activity contributes to more efficient cycling.

The quantity of muscle activity is highly influenced by workload. As workloads increase, the activity level of the VM, MG, Sol, GM, gluteus medius, RF, BF and ST also increases (Ericson et al., 1985). In addition, both power output and VL activity increased throughout a 40 km time trial (Bini et al., 2008), while in a 30 minute time trial, with no time effect on power output, there was no significant change in the activity level of VM, RF, BF or MG (Duc et al., 2005). The response to altered workloads is not uniform across all muscles. Some muscles such as the GM are more susceptible to changes in

load, while others like VL, VM, MG and LG show less variation with different workloads (Ericson, 1986; Ericson et al., 1985).

1.3 Pedal Forces

One approach to maximize cycling efficiency is to increase mechanical work without increasing muscle activity. The direction, magnitude and duration of forces applied to the pedal are affected by the coordination of leg muscle activation, which is reflected in the mechanical work and power output of a cyclist. Force applied to the pedals in a direction perpendicular to the crank arm at every point in the pedal cycle would produce more power; however, anatomical constraints suggest that muscles may be more effective in delivering forces in non-optimal directions relative to the pedals (van Ingen Schenau et al., 1992). In short sprints at maximal power output cyclists display a positive contribution of force during the upstroke (Martin & Brown, 2009), whereas they show a negative force in the upstroke during prolonged cycling (Sanderson & Black, 2003). This implies that when power output is the primary goal, forces applied perpendicular to the crank arm for more of the pedal cycle are more effective, whereas when efficiency is important in longer cycling events, other force application strategies are more effective. Therefore, there exists a balance between muscle activity and the direction and magnitude of the applied force that will produce a high power output with minimal energy cost thereby maximizing cycling efficiency.

Instrumented pedals are used to determine the total, effective and ineffective pedal forces. The effective force is the force applied normal to the crank arm and is often used to calculate pedal effectiveness or the index of effectiveness, which is the ratio of the effective force to the total force. In cycling, the primary application of force that contributes to positive work occurs in the downstroke (from 0º, when the crank arm is at the top dead centre (TDC) of the rotation, to 180º) (Coyle et al., 1991; Hug et al., 2008; Sanderson, 1991; Zameziati et al., 2005). Investigations of the downstroke reveal consistency in the force pattern between subjects (Coyle et al., 1991; Hug et al., 2008; Patterson et al., 1983; Sanderson, 1991) independent of training status. During the upstroke (from 180º back to 0º) some cyclists display resistive forces (Hug et al., 2008; Patterson & Moreno, 1990; Patterson et al., 1983; Rossato et al., 2008; Sanderson, 1991; Zameziati et al., 2005), others contribute very little or no force (Coyle et al., 1991; Sanderson, 1991), and some show increased positive work (Coyle et al., 1991;

4

Zameziati et al., 2005). The variation in pedal force application requires different contributions of muscle activity and should be detected in the muscle coordination patterns, which will have an effect on the mechanical power output and the metabolic costs of cycling. Mornieux et al. (2006) found that net muscular efficiency increased with pedal effectiveness of the downstroke during steady state cycling. Since they measured oxygen consumption without including muscle activity, the relationships between muscle coordination and either pedal effectiveness or muscular efficiency cannot be determined. In addition, the location in the pedal cycle where pedal effectiveness changed cannot be established since the downstroke was examined as a single unit.

Cyclists tend to intensify the angular impulse (Coyle et al., 1991; Kautz et al., 1991; Sanderson & Black, 2003; Sanderson, 1991; Zameziati et al., 2005) and vertical forces (Coyle et al., 1991; Kautz et al., 1991; Sanderson, 1991) during the downstroke as workload increases. Elite competitive cyclists even employ higher vertical forces during the downstroke compared to good competitive cyclists, despite decreased pedal effectiveness, resulting in increased total power output (Coyle et al., 1991). The increased vertical forces utilize the GM, VL and VM during the downstroke, where the pedal effectiveness is at its maximum, potentially reducing the muscle activity required for a given power output. In addition, in cycling trials to exhaustion decreased effective force during the upstroke and increased dorsi-flexion in the ankle resulted in an earlier switch to pulling back on the pedal at the end of the test (Sanderson & Black, 2003). Some cyclists even showed increased effectiveness around the top of the pedal cycle (Kautz et al., 1991; Sanderson, 1991). This and the earlier transition from pushing down to pulling back on the pedal are partially explained by an increased dorsi-flexed ankle position causing a greater application of horizontal force around the top of the cycle and during the downstroke (Kautz et al., 1991; Sanderson & Black, 2003). This results in more GM and knee extensor activation around the top of the pedal cycle and allows for force application for more of the downstroke.

1.4 Cycling Time Trial Pacing

The pacing strategy used in time trial cycling also influences the muscle coordination patterns. Pacing strategies disperse the workload required to complete a cycling event in different ways (see review (Abbiss & Laursen, 2008)), which affects both the power output and fatigue levels, both of which have an effect on muscle coordination

(Hug & Dorel, 2009). There is conflicting evidence regarding the interaction between pacing and muscle activation. Hettinga (2006) found that VL and BF activity increased throughout a 4,000 m time trial despite negative (increasing power output), positive (decreasing power output) and even (constant power output) power output pacing strategies (Abbiss & Laursen, 2008). Conversely, St Clair Gibson (2001) found that RF activity declined in conjunction with power output in a 100 km time trial with high intensity bouts. With only RF measured they speculated that other muscles could have acted in compensation thereby altering muscle coordination.

1.5 Purpose

This study aims to develop a better understanding of leg muscle coordination, both in the field and in the laboratory, by examining factors that affect muscle coordination and efficiency in cycling. The indoor portion of the study examines the interactions between coordinated muscle recruitment and the total amount of muscle activity, power output, cadence, direction and amplitude of pedal forces, hip, knee and ankle joint angles and overall mechanical efficiency at a variety of workloads. This will identify muscle coordination patterns utilized at the highest and lowest power outputs, total muscle activities and overall mechanical efficiencies as well as determine the pedal forces and kinematics present in each situation. The outdoor portion of the study investigates the relationships between muscle coordination patterns and power output, cadence, total muscle activation, overall mechanical efficiency, terrain and distance during a time trial. This will ascertain muscle coordination patterns used to produce the extremes of power output, total muscle activity and overall mechanical efficiency and discover the impact of terrain, distance and pacing. The study was not designed to compare indoor and outdoor cycling directly, but highlights commonalities between the two environments where possible. Predicted outcomes include the following:

- Pedal effectiveness will be significantly associated with the muscle coordination patterns during indoor cycling.
- Overall mechanical efficiency will be significantly associated with the muscle coordination patterns during both indoor and outdoor cycling and coordination patterns used for high and low efficiency cycling will be identifiable.

- The muscle coordination patterns will have a significant effect on and relationship with power output, cadence, pedal forces and kinematics in indoor cycling.
- The muscle coordination patterns will have a significant effect on and relationship with power output, cadence, slope and distance in outdoor time trial cycling.
- Greater VL and VM activity will occur with increased power output and earlier onset of muscle activity in all muscles will occur with increased cadence in both indoor and outdoor cycling.

CHAPTER 2: INDOOR STUDY

2.1 Introduction

Few studies have compared and connected variations in muscle activity to changes in efficiency during cycling. In particular, research relating muscle activity to the factors affecting mechanical work such as pedal forces and kinematics is limited. This is an important area of research to further the understanding of how muscles work together in a coordinated fashion to produce movement. Specifically, whether individual muscles or coordinated recruitment of multiple muscles are responsible for the power output and overall mechanical efficiency used in cycling and how these affect or are affected by factors such as pedal forces and kinematics. Hug (2008) showed that a large amount of variation in the muscle activity between different subjects is not accompanied by significant amounts of variation in the pedal forces. This implies that different combinations of muscle activity can produce similar forces on the pedals, but does not clarify which recruitment patterns maximize the cycling efficiency ratio by minimizing the metabolic costs. Muscles such as RF and BF, which display large amounts of variability in the timing of muscle activation (Ryan & Gregor, 1992), may help clarify differences in metabolic costs as they explain the disparity in total leg muscle activity. Also shifts in the timing of LG, MG and TA relative to the pedal cycle, as they fatigue in exhaustive cycling (Dorel et al., 2009), results in limited range of motion and increased ankle dorsi-flexion altering the direction of force application on the pedals (Sanderson & Black, 2003). Fatigue of the lower leg and primary power producing muscles (VL and VM) and the resulting change in ankle joint range of motion partially explains the increased and altered involvement of GM and BF seen at increased workloads. These changes have a direct effect on the direction of applied force on the pedals with increased force, force effectiveness and GM muscle activity around the top of the pedal cycle and more force, force effectiveness and BF muscle activity around the bottom of the pedal cycle (Sanderson & Black, 2003).

It is unclear how these changes in muscle coordination patterns and their associated pedal forces combined to affect cycling efficiency. Muscle efficiency has

been shown to increase with pedal effectiveness during the downstroke in steady state cycling (Mornieux et al., 2006). Also, pedal effectiveness increases with power output primarily in the upstroke during short sprint cycling (Martin & Brown, 2009), while it decreases largely in the upstroke during prolonged cycling (Sanderson & Black, 2003). This implies that there is more relative muscle activation during the upstroke at the highest power outputs, whereas there may be relatively more muscle activity of the opposite leg (which is in the downstroke portion of the cycle) to overcome the resistive forces in longer duration cycling. Maximum pedal force effectiveness and minimum amount and duration of muscle activity may be effective for high power output or long duration cycling respectively, but they are unlikely to occur simultaneously in cycling. Therefore, this study aims to identify the balance of muscle timing and coordination, pedal force application and total muscle activity that maximizes cycling efficiency.

2.2 Methods

2.2.1 Protocol and Data Acquisition

Nine experienced competitive male cyclists (age 41.8 ± 2.7 years (mean ± standard error of the mean (SEM)); mass 77.2 ± 2.2 kg; height 1.81 ± 0.01 m; maximal oxygen consumption (O_{2max}) 64.65 ml/kg/min; distance cycled per year 9428 ± 1913 km) participated in the study. The participants gave their informed written consent and all procedures were approved by the Ethics Committee in accordance with the Office of Research Ethics at Simon Fraser University.

One week prior to the main testing date the participants performed an incremental cycling test to exhaustion to determine O_{2max}. Oxygen and carbon dioxide gas exchange were sampled breath by breath using a metabolic cart (Vmax 229, Sensormedics, Yorba Linda, California) and the participants were instructed to maintain a constant freely chosen cadence throughout the test which was used in the main testing protocol. For the main test the participants cycled in clipless pedals at power outputs representing 25, 40, 55, 60, 75 and 90% O_{2max} on an indoor trainer (SRM, Jülich, Germany). Resistances were presented in two groups, group 1: 25, 40 and 55% O_{2max} and group 2: 60, 75 and 90% O_{2max} and repeated in two blocks as block 1: group 1, group 2 and block 2: group 2, group 1. Resistances within the groups were presented in

random order for 3 min each and the blocks were separated by a 5-min rest period. The final 30 s of data from each 3 min trial was used for analysis.

Oxygen and carbon dioxide gas exchange, respiratory quotient (RQ), power output, cadence, heart rate, kinematics, pedal forces and EMG were continuously monitored. EMG was measured from the TA, MG, LG, Sol, VM, RF, VL, BF, ST and GM using bipolar Ag/AgCl surface electrodes (10 mm diameter, 21 mm spacing). The EMG electrodes were placed on the right leg after the removal of hair and cleaning with isopropyl wipes. EMG signals were amplified (Biovision, Wehrheim, Germany) and recorded through a 16-bit A/D converter (USB-6210, National Instruments, Austin, TX). Normal and tangential forces applied to the pedals were measured using a pedal dynamometer (VélUS, Department of Mechanical Engineering, Sherbrooke University, Canada) and resolved into normal and tangential forces relative to the crank arm. Cycling cadence, total power output and the power output from each pedal were also calculated from the pedal dynamometers.

Saggital kinematics of the right leg and foot were measured at 100 Hz using an optical motion capture system (Optotrak, Northern Digital Inc., Waterloo, Canada). Two sets of three LED markers were placed on rigid bodies that were attached to the thigh and shank and three LED markers were placed on the cycling shoe. LED markers were then placed on the lateral femoral condyle and lateral malleolus for a standing trial prior to the test in order to obtain their orientation relative to the rigid bodies: these markers were removed for the test and the position of the knee and ankle joints tracked as virtual markers. Hip flexion was measured using a twin-axis goniometer (SG 150, Penny & Giles Biometrics Ltd., UK) attached above and below the greater trochanter. Heart beats were measured using a Polar T31 transmitter and a wireless receiver (Polar Electro Oy, Finland). The EMG, pedal force, hip kinematics and heart rate data were recorded at 2000 Hz and synchronized to the ankle and knee kinematics.

2.2.2 Data Analysis

The EMG signals were resolved into EMG intensities by wavelet techniques using ten wavelets (k=1-10; (von Tscharner, 2000)). The EMG intensity across this frequency band (approximately 11-432 Hz; (von Tscharner, 2000)) was interpolated to 100 evenly spaced points for each pedal cycle, starting at TDC. The EMG intensities were normalized to the mean intensity for each participant for each muscle. The total

EMG intensity, I_{tot}, was given by the sum of the EMG intensities across all muscles for each pedal cycle. For ease of description the pedal cycle was broken into four segments: quadrant 1 (Q1) was the first 90º of forward pedalling starting at TDC, Q2 was from 90º to 180º of the crank arm rotation, Q3 was from 180º to 270º and Q4 was from 270º back to TDC (Figure 1). The downstroke comprises Q1 and Q2 and the upstroke comprises Q3 and Q4.

Due to the large multivariate data sets obtained in this experiment principal component (PC) analysis was used to reduce the number of variables and extract the important features. The EMG intensities from all ten muscles were used to construct a pattern of muscle coordination for each pedal cycle and PC analysis was used to identify predominant coordination patterns during the cycling (Wakeling & Horn, 2009). In short, data from all the cycles were placed into a $P \times N$ matrix **A**, where $P = 1000$ samples per pattern (10 muscles $\times$ 100 EMG intensities per cycle), and $N = $ the number of pedal cycles analyzed (all subjects and all trials). The covariance matrix **B** was calculated from the data matrix A, and the PC weightings, $I_{PC,W}$, were determined from the eigenvectors ζ of covariance matrix B. The importance of each PC was given by the eigenvalue for each eigenvector-eigenvalue pair with the greatest absolute eigenvalues corresponding to the main PCs. The relative proportion of the coordination patterns explained by each PC was given by $\zeta'B\zeta$. The loading scores for each PC, $I_{PC,LS}$, for the N pedal cycles were given by $\zeta'A$. With PC1 representing the dominant coordination pattern for all trails and all participants, the contribution of each $I_{PC,LS}$ relative to $I_{PC1,LS}$ for all pedal cycles was used in the analysis by normalizing each $I_{PC,LS}$ to $I_{PC1,LS}$ ($\hat{I}_{PC,LS}$). This implies that for a ratio of one there was an equal amount of a particular $I_{PC,LS}$ to $I_{PC1,LS}$ even though the $I_{PC,W}$ may represent only a small percentage of the entire EMG signal.

Effective and ineffective forces (F) relative to the crank arm and the limb kinematics (hip, knee and ankle angles) were interpolated into 100 evenly spaced points per pedal cycle. The pedal effectiveness, η_P, (also known as the index of effectiveness) was determined as the ratio of effective to resultant force on the crank arm. PCs for the pedal forces, F_{PC}, for the pedal effectiveness, $\eta_{P,PC}$, and for the limb kinematics, K_{PC}, were calculated in a similar manner to the PC analysis for the EMG intensities. A significant positive relationship between I_{tot} and the metabolic power using the same methods has previously been reported (r=0.86; (Wakeling et al., 2011)) so I_{tot} was used as an instantaneous, cycle-by-cycle estimate of metabolic power. The overall

11

Figure 1. Principal component weightings for the EMG intensity, pedal forces and kinematics in the indoor trial.
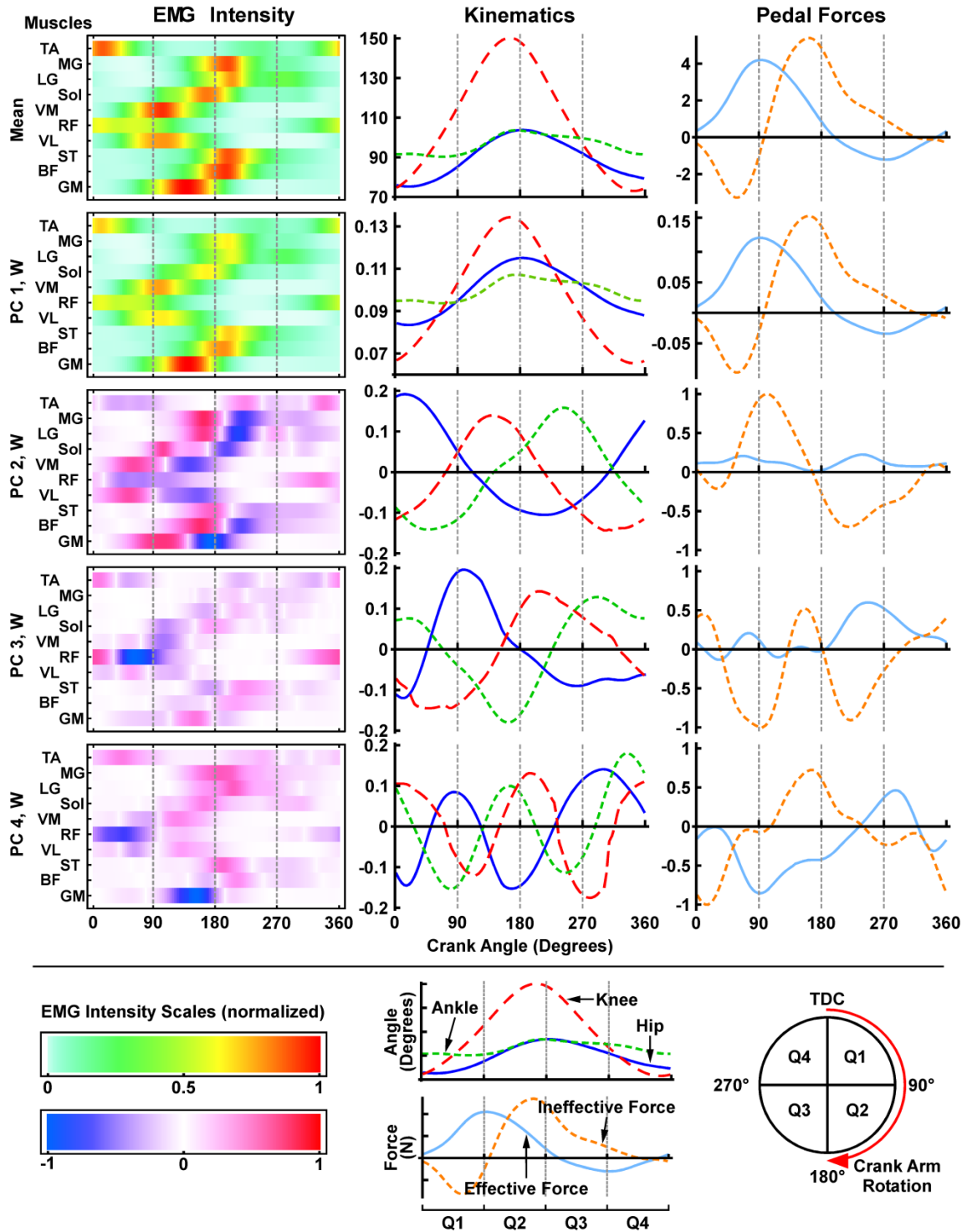
The first row represents the mean EMG intensity, ankle (green line), knee (red line) and hip (blue line) joint angles and effective (normal to the crank arm; light blue line) and ineffective (tangential to the crank arm; orange line) forces per pedal cycle. Subsequent rows are representations of the first four PC weightings (PC, W). Figure legends and scales are shown at the bottom.

mechanical efficiency, η_O, is the ratio of mechanical power output to the metabolic power per pedal cycle and therefore was estimated by the ratio of the mechanical power output to I_{tot}. The mechanical power output used both to calculate η_O and in the statistical analysis was normalized to the mean power output for each subject.

2.2.3 Statistics

The most important features of the coordination patterns for the EMG intensities were explained by their most PCs. Using general linear multivariate analyses of covariance (MANCOVA) the relationships were determined between the muscle coordination patterns and the following factors: subject, block, trial, cadence, pedal forces, limb kinematics and η_P. Also the effect of subject, trial, block, cadence, $I_{PC,LS}$s, $\eta_{P,PC,LS}$s, $K_{PC,LS}$s and $F_{PC,LS}$s on power output, I_{tot} and η_O was determined using MANCOVA. The first ten $I_{PC,LS}$s ($I_{PC1,LS}$ and $\hat{I}_{PC,LS}$ for all other PCs) were tested individually as the dependant variables with subject as a random factor, trial and block as fixed factors, and cadence, $\eta_{P,PC}$s, K_{PC}s and F_{PC}s as covariates. Additionally, power output, I_{tot} and η_O were analyzed individually as dependent variables with subject as a random factor, trial and block as fixed factors, and power output, cadence, $I_{PC,LS}$s ($I_{PC1,LS}$ and $\hat{I}_{PC,LS}$ for all other PCs), $\eta_{P,PC,LS}$s, I_{tot}, $K_{PC,LS}$s and $F_{PC,LS}$s as covariates (with the exception that the dependant variable was not included as an independent variable). Statistical tests were considered significant at p≤0.05.

The EMG intensities were reconstructed from the sum of the products of the PC weights and their loading scores ($\sum I_{PC,W} I_{PC,LS}$) for each pedal cycle, using the first 10 PCs. The effect of muscle coordination on power output, I_{tot} and η_O was visualized in the following manner. The EMG coordination patterns were reconstructed using the first 10 PCs that describe the major features of the coordination. For each mechanical factor (power output, I_{tot} or η_O) if the $I_{PC,LS}$ had no significant effect on the mechanical factor (as determined from the MANCOVA) then the mean $I_{PC,LS}$ was used. Alternatively, if the $I_{PC,LS}$ showed significant covariance with the mechanical factor then the pedal cycles were ranked by that factor and the mean $I_{PC,LS}$ from either the top or bottom 100 cycles were taken from the rank. Thus, the major features of the muscle coordination that occurred with the highest or lowest of each factor (e.g. power output) were reconstructed. Patterns of pedal forces, η_P and limb kinematics were similarly reconstructed from their first five PCs. Values are reported as mean ± SEM.

2.3 Results

The mean cadence across all subjects and trials was 94.95 ± 0.08 rpm and there was no significant difference in mean cadence between conditions or between blocks. EMG intensities varied in timing and amplitude with each pedal cycle. Heart rate, EMG intensities and mechanical power output increased in conjunction with resistance. The 25, 40, 55 and 60% $\dot{V}O_{2max}$ trials had RQ values less than 1 while the 75 and 90% $\dot{V}O_{2max}$ trials were above 1 indicating a greater contribution of the anaerobic energy system for the group 2 trials (Figure 2). Despite this the participants completed the protocol and therefore did not experience failure due to fatigue. There was a significant decrease in RQ and a significant increase in heart rate from block 1 to block 2, yet no significant difference in power output, I_{tot}, or η_O between blocks.

Figure 2. Total EMG intensity for each indoor condition (25, 40, 55, 60, 75 and 90% O2max) and each muscle (TA, MG, LG, Sol, VM, RF, VL, ST, BF and GM).

	Trial (%$\dot{V}O_{2max}$)					
	25	40	55	60	75	90
Cadence (rpm)	94.8 ± 1.1	94.1 ± 1.2	94.9 ± 1.1	94.9 ± 1.2	94.5 ± 1.1	95.3 ± 1.2
Power (Watts)	103.5 ± 2.3	155.6 ± 3.7	204.0 ± 5.4	227.0 ± 5.9	273.0 ± 6.4	325.7 ± 8.7
Total Intensity (I_{tot})	559.1 ± 42.8	704.8 ± 50.3	906.7 ± 70.4	968.4 ± 65.0	1339.5 ± 103.0	1833.7 ± 128.4
Overall Efficiency (η_O)	0.0915 ± 0.0071	0.1056 ± 0.0075	0.1063 ± 0.0077	0.1085 ± 0.0071	0.0947 ± 0.0068	0.0834 ± 0.0061
RQ	0.91 ± 0.02	0.90 ± 0.01	0.95 ± 0.01	0.96 ± 0.02	1.04 ± 0.02	1.16 ± 0.02
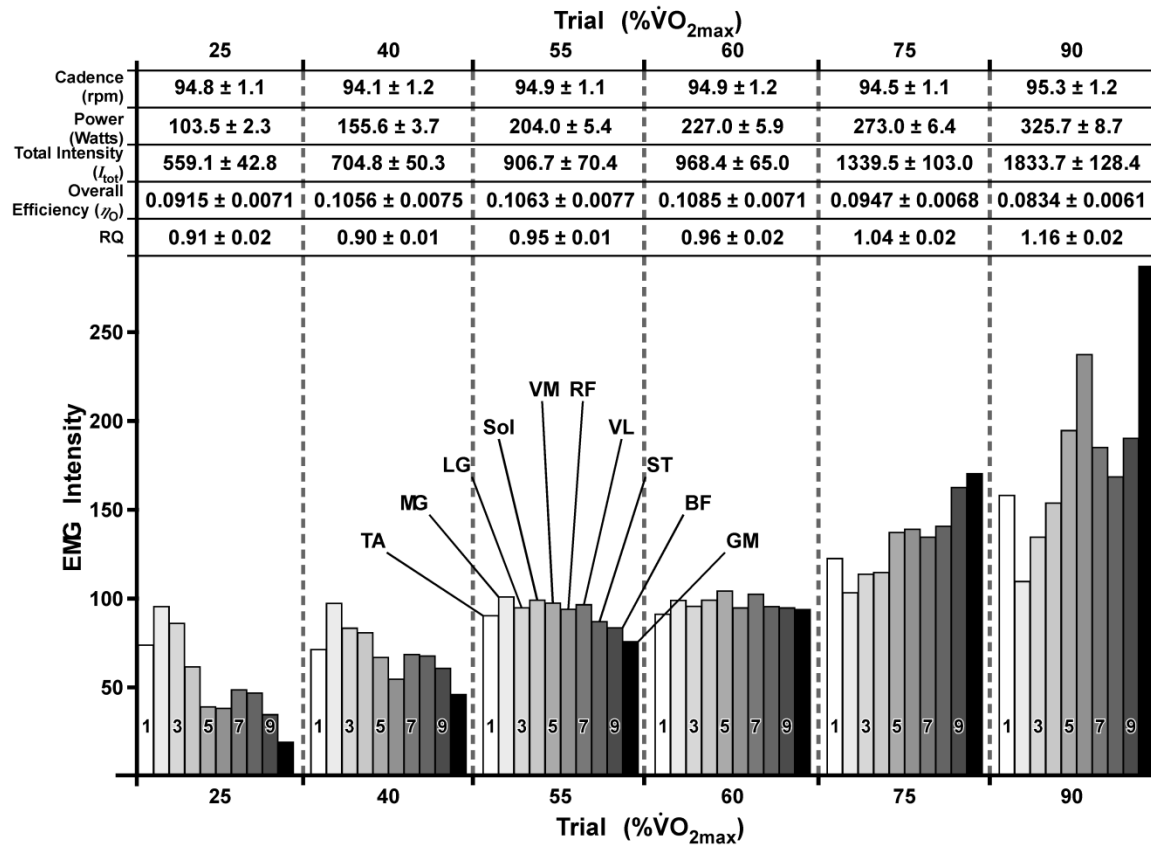
The top rows show the mean ± SEM power output, cadence, total muscle intensity, overall mechanical efficiency and respiration quotient (RQ) for each condition.

14

The first ten $I_{PC,W}$s explained over 81% of the coordination patterns. $I_{PC1,W}$ explained 55.4% of the signal and was similar to the mean muscle intensity pattern (Figure 1). $I_{PC1,LS}$ was correlated with the mechanical power output (r=0.84; Figure 3a), I_{tot} (r=0.98; Figure 3b), η_O (r=0.60; Figure 3c) and η_P (r=0.76). $I_{PC2,W}$ explained 7% of the coordination patterns and showed positive intensity for all muscles earlier than each muscles' peak intensity in $I_{PC1,W}$ and negative intensity at or just after the peak intensity of $I_{PC1,W}$ (Figure 1). $\hat{I}_{PC2,LS}$ was correlated with cadence (r=0.94). GM had the largest range of mean total EMG intensity per pedal cycle between conditions followed by RF, BF, VM and VL (Figure 2). MG showed very little change between conditions with LG, Sol and TA displaying only a slightly greater range (Figure 2).

2.3.1 Power Output

The power output from the right pedal was an excellent predictor of the total mechanical power output (r=0.99) and so the results below focus primarily on the power output from the right pedal (normalized) as the EMG and kinematics were measured from this leg. $I_{PC1,W}$ accounted for the general muscle coordination pattern and was very similar to the mean coordination pattern (Figure 1). $I_{PC4,W}$ showed a general positive weight for EMG intensity for TA, MG, LG Sol, ST and BF and negative weights for GM and RF (Figure 1). $\hat{I}_{PC4,LS}$ was negatively correlated with power output (r=-0.84), and decreased at higher powers (r=-0.81; Figure 3d). Thus, at lower powers there was relatively smaller contribution of GM and RF and relatively greater contribution of TA, MG, LG Sol, ST and BF to the reconstructed coordination pattern; this situation was reversed at higher powers (Figure 4). Additionally, the reconstructed coordination patterns for higher power outputs were larger in amplitude with VM, VL and BF displaying a shift to earlier peak intensities than for lower power outputs (Figure 4).

The first three $F_{PC,W}$s explained over 98% of the signal (Figure 1) with $F_{PC1,LS}$, $F_{PC2,LS}$ and $F_{PC3,LS}$ correlated with power output (r=0.74, 0.61 and 0.70 respectively). The reconstructed forces showed that higher power outputs were associated with higher effective force during the downstroke and more negative effective force during the upstroke (opposite of the direction of crank arm rotation) (Figure 5). The mean η_P for the pedal cycle had a strong positive relationship with power output (r=0.89). The $\eta_{P,PC1,W}$

Figure 3. Indoor relationships between power output, total muscle intensity, overall mechanical efficiency (power output/ total muscle intensity) and the loading scores for the EMG intensities ($\hat{I}_{PC4,LS}$ represents the ratio of $I_{PC4, LS}/ I_{PC\,1,\,LS}$ (d, e and f) and shows the relative contribution of $I_{PC4,\,LS}$ to $I_{PC\,1,\,LS}$).
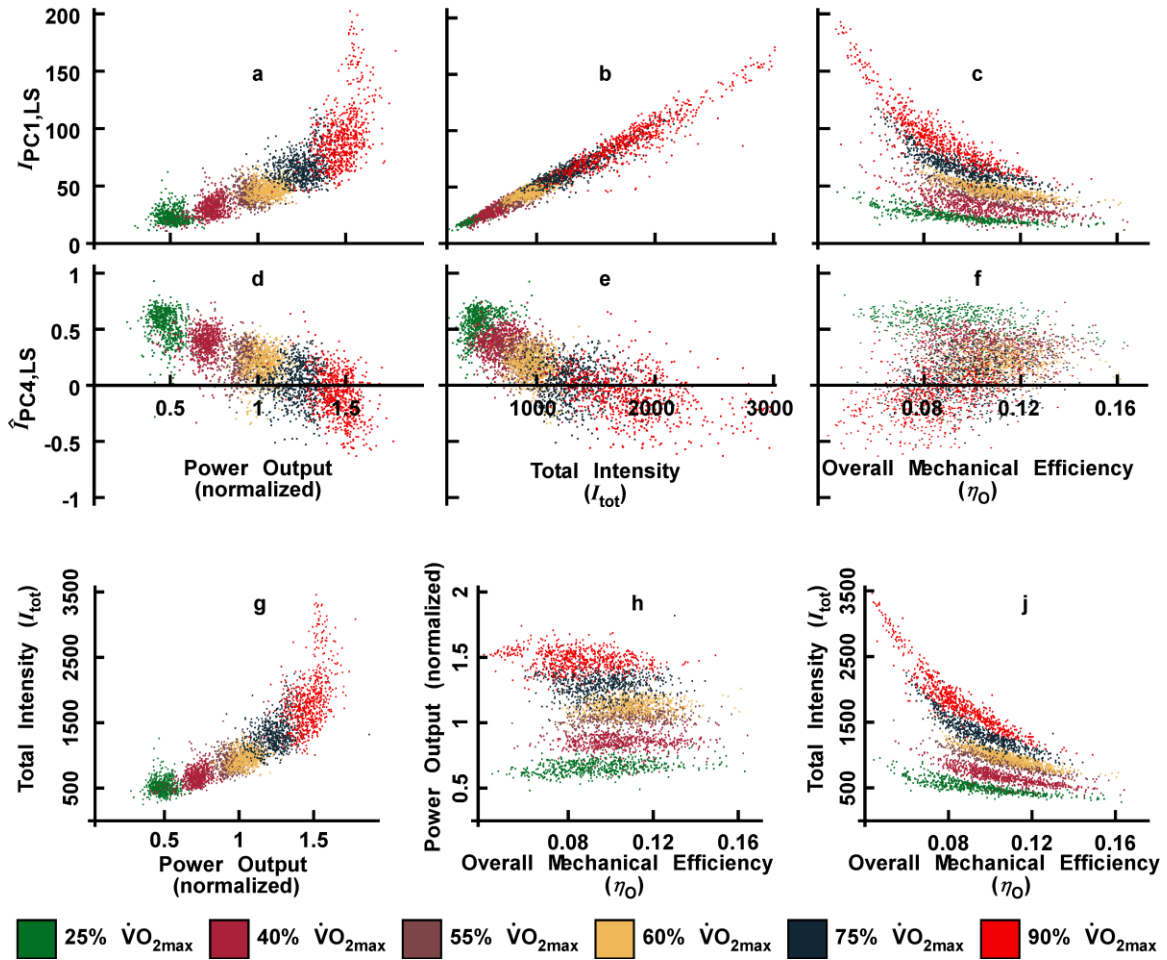
explained 93% of the η_P signal, however $\eta_{P,PC1,LS}$ showed a low correlation with power (r=0.22). The reconstructed η_P showed that the increased η_P at higher powers resulted from an increased pedal effectiveness during the upstroke and across TDC (Figure 5).

The reconstructed hip angles for high power output were smaller in Q4 and Q1 and larger in Q2 and Q3 than for the low power output, whereas the knee angles were similar throughout (Figure 5). The ankle angles for the high power outputs were 5-14º more dorsiflexed than for the low power outputs throughout the pedal cycle (Figure 5).

Figure 4. Indoor coordination patterns reconstructed from the PC analysis for all muscles for power output, total EMG intensity and overall mechanical efficiency.
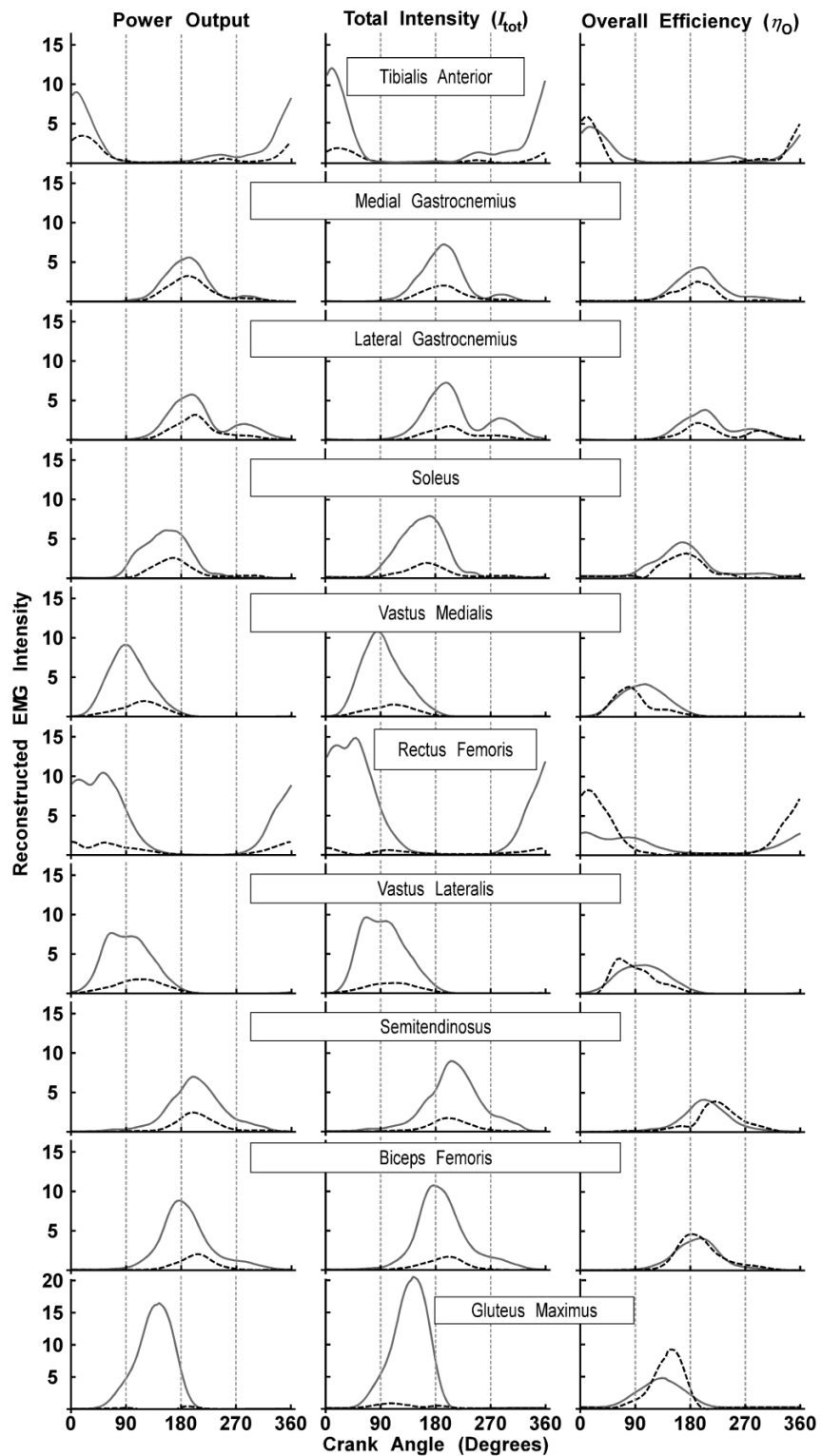
The figures show high (grey line) and low (black dashed line) states of power output, total EMG intensity and overall mechanical efficiency. The first ten PCs were used for each reconstruction.

Figure 5. **Indoor pedal forces, pedal effectiveness and saggital plane joint angles reconstructed from the PC analysis.**
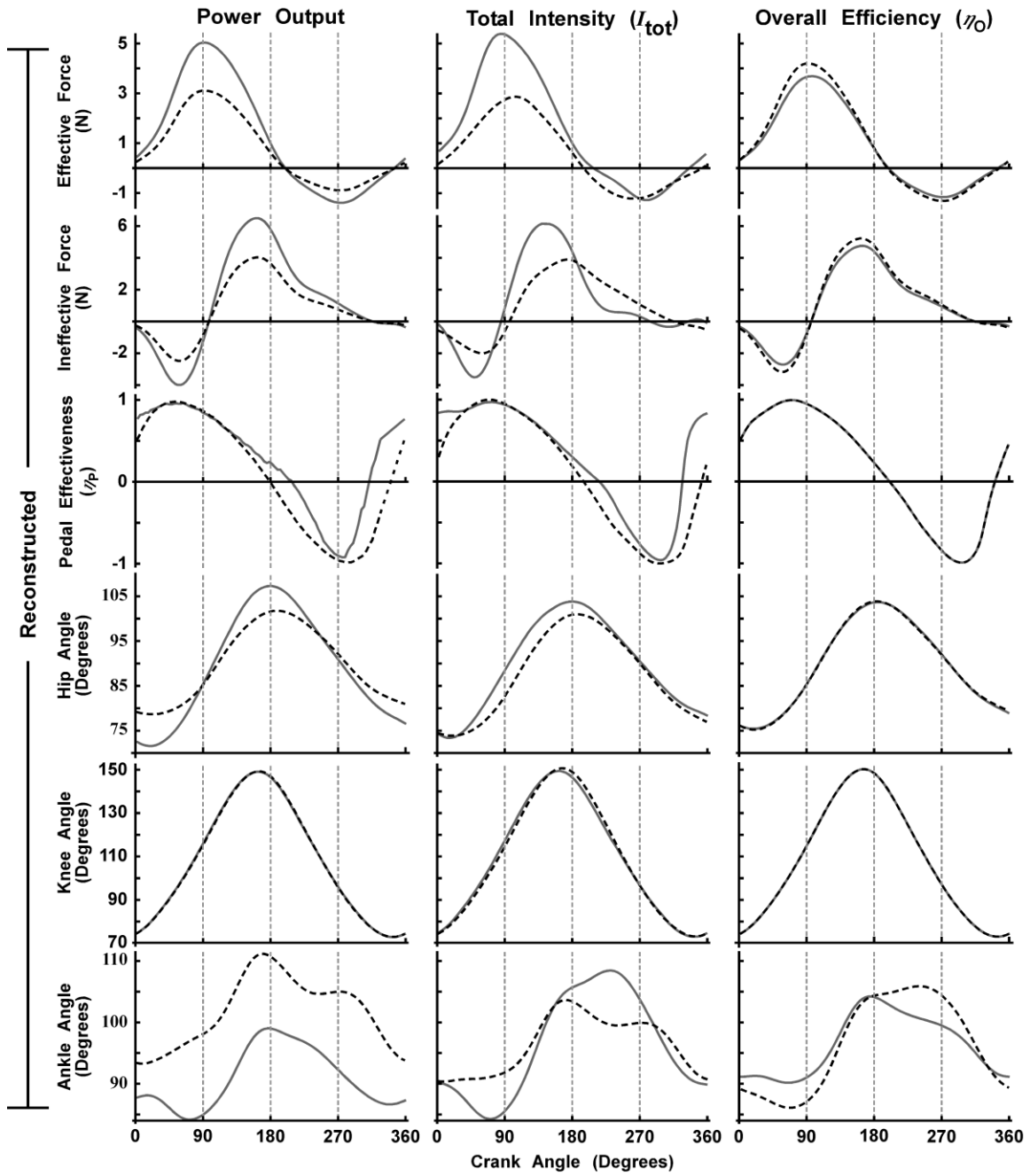
Figures show high (grey line) and low (black dashed line) states of power output, total EMG intensity and overall mechanical efficiency. The first five PCs were used for each reconstruction.

2.3.2 Total EMG Intensity, I_{tot}

I_{tot} correlated strongly with power output (r=0.86; Figure 3g) and so many of the relations between muscle power output and muscle coordination were matched by similar relations between I_{tot} and coordination. I_{tot} correlated positively with $I_{\text{PC1,LS}}$ (r=0.98; Figure 3b) and negatively with both $I_{\text{PC4,LS}}$ and $\hat{I}_{\text{PC4,LS}}$ (r=-0.66 and -0.74 respectively; Figure 3e). The reconstructed coordination patterns showed greater EMG intensity for all muscles when at high I_{tot}, with the greatest increase being in RF and GM (Figure 4). Additionally, high I_{tot} was associated with timing advances for VM and VL in the downstroke and BF at the bottom of the pedal cycle (Figure 4).

High I_{tot} was associated with a larger peak effective force during the downstroke and similar effective force during the upstroke (Figure 5). The ineffective force was more negative in Q1, more positive in Q2 (when it reached its maximum values) and smaller throughout the upstroke (Figure 5). The primary difference in η_{P} occurred at the top of the pedal cycle where η_{P} was elevated for higher total intensity (Figure 5). Hip angles were larger throughout the pedal cycle for higher I_{tot} compared to lower I_{tot} with the largest difference of approximately 6° during the downstroke portion of the pedal cycle (Figure 5). Knee angles were similar for high versus low I_{tot} (Figure 5), while the ankles were more dorsiflexed in Q1, Q2 and Q4 and more plantarflexed in Q3 for high I_{tot} (Figure 5).

2.3.3 Overall Efficiency, η_{O}

The 55% and 60% O_{2max} trials showed the highest levels of η_{O} with the 90% and 25% O_{2max} trials significantly lower (Figure 2). As η_{O} increased, I_{tot} decreased (Figure 3j) while power output remained reasonably constant (Figure 3h) which was particularly apparent in the 90% O_{2max} condition. There was a significant correlation between η_{O} and $I_{\text{PC1,LS}}$ (r=-0.60; Figure 3c), and also $\hat{I}_{\text{PC4,LS}}$, $\hat{I}_{\text{PC5,LS}}$, $\hat{I}_{\text{PC7,LS}}$ and $\hat{I}_{\text{PC8,LS}}$ and therefore the overall efficiency was strongly related to the muscle coordination patterns. At low η_{O} there were lower EMG intensities for MG, LG and Sol, greater EMG intensity for GM in the second half of Q2, greater RF and TA intensities across the top of the pedal cycle, earlier peak VM, VL and BF and later peak ST intensities (Figure 4).

There was little difference in pedal forces and no difference in η_{P} between high and low η_{O} (Figure 5). The hip and knee angles showed negligible difference between

high and low η_O. The ankle angles were more plantarflexed during the downstroke and more dorsiflexed during the upstroke for the high η_O (Figure 5).

2.4 Discussion

This study has shown that there are significant associations between muscle coordination, forces acting on the pedals, kinematics, mechanical crank power, total EMG intensity and overall mechanical efficiency.

2.4.1 Pedal Effectiveness, η_P, and Pedal Forces, *F*

As with previous studies, the mean η_P for the entire pedal cycle increased with workloads (Rossato et al., 2008; Sanderson, 1991), however it was not a good indicator of η_O. With the large time-varying fluctuation in effective force throughout the pedal cycle, instantaneous η_P from the $\eta_{P,PC}$s was utilized in the analysis of total muscle intensity, power output and η_O. $F_{PC1, W}$ explained 98% of the pedal forces, so the pattern of pedal force application was very consistent amongst cyclists (Hug et al., 2004), with the primary differences arising from changes in amplitude. This study supported previous reports since as the workload increased there was an increase in the effective force during the downstroke (Coyle et al., 1991; Kautz et al., 1991; Sanderson, 1991), a more negative effective force during the upstroke and more positive ineffective force in Q2, Q3 and Q4 (positive ineffective force is directed away from the centre of crank arm rotation) (Figure 5; (Coyle et al., 1991)).

2.4.2 Muscle Activation

The primary pattern of EMG intensity ($I_{PC1,W}$) related to the general coordination pattern required for cycling and was similar to the mean coordination pattern for all participants in all trials (Figure 1). The significant correlation between $I_{PC1,LS}$ and I_{tot} indicated that the EMG intensity showed general increases as the trials intensified (Figure 3b). In terms of specific muscles, GM had the largest rise in muscle activity from low to high resistance (Figure 2) and played a significant role in high power production which was largely due to the relative decrease in $\hat{I}_{PC4,LS}$ (Figure 3d). Ericson (1986) found GM to have low peak activity levels relative to maximum voluntary contractions (approximately 10% and 40% for 120 W and 240 W conditions respectively) thereby not contributing as much to power production as found here. In this study the mean power

output for the 90% O_{2max} condition was substantially higher at 326 ± 9 W and there was a considerable rise in GM intensity between all conditions (Figure 2). Therefore there is evidence that GM was active at a high percentage of its maximum and supports its role as a contributor to high power production (Ryan & Gregor, 1992).

RF and TA also showed increases in EMG intensity across the top and early part of the pedal cycle with rising power outputs (Figure 4), although given the electromechanical delay their primary application of force would occur during the first half of Q1. These muscles play a role in moving the pedal over the top and at the start of the new pedal cycle to apply force to the pedal during the downstroke (Ericson, 1986; Neptune et al., 1997). RF crosses two joints and performs dual functions of flexion of the hip and extension of the knee, while TA acts to dorsiflex the ankle. Muscles crossing two joints are thought to transfer force between the joints and control the direction of force application on the pedal (van Ingen Schenau et al., 1992). Given that RF and TA were the only muscles demonstrating noticeable amounts of muscle activity across TDC and through the early portion of Q1 (Figure 1), there is evidence that both were controlling the direction of force. The kinematic traces showed that the hip was undergoing a small amount of flexion, the knee was extending and the ankle angle was not changing across TDC (Figure 1), yet there was very little force acting at the pedal (Figure 1). Considering the lack of muscle activation in VM and VL, RF could have been acting to both flex the hip to avoid adding resistance to the pedals from the weight of the leg and extending the knee. As the knee was extending in Q1, TA maintained ankle dorsiflexion in order to orient the pedal in a direction that would allow the force to be applied to the crank during the downstroke. Since the EMG intensities are normalized for each muscle the EMG intensity can only be determined relative to itself. This means that the high levels of EMG intensity for TA and RF at TDC and in Q1 may not result in much force, but were their maximum values in the pedal cycle. Although, as with GM, RF exhibits significantly more muscle activity relative to maximum voluntary contraction from 120 W to 240 W (Ericson, 1986). Aside from GM, RF muscle activity increased more than any other muscle from the 25% to the 90% O_{2max} condition (Figure 2). This suggests that RF may have been contributing significant amounts of force to the early portion of the pedal cycle at high resistances. Whether producing a lot or very little force RF and TA appear to be the keys to power production by initiating knee extension and maintaining appropriate joint angles.

21

VL and VM have been shown to be large power producing muscles during the downstroke (Bini et al., 2008; Ericson, 1986; Ryan & Gregor, 1992). This study did not find the same increase in EMG intensity for VL and VM as for GM and RF at higher workloads, yet both were highly active during the downstroke when most of the power was being produced (Figure 4). This adds more evidence that these muscles are big contributors to the power output regardless of the resistance (Ericson, 1986). At the bottom of the pedal cycle during the transition from the downstroke to the upstroke the ankle plantar flexors (MG, LG and Sol) as well as the knee flexors (ST and BF) showed the most activity in the primary muscle coordination pattern ($I_{PC1,W}$; Figure 1). The Sol displayed the greatest EMG intensity in the second half of Q2 before the bottom of the pedal cycle when GM was also at its maximum, whereas LG and MG showed greatest intensity just after the bottom. This could be because Sol helped to stabilize the ankle joint and transfer power produced by GM to the pedal, similar to the simulation study findings by Neptune (2000). Sol is a single joint muscle with a higher percentage of slow type muscle fibres than MG and LG (Johnson et al., 1973) and is used more at high resistances (Wakeling & Horn, 2009). It is therefore better suited to stabilize and plantar flex the ankle joint to contribute to the pedal force through the lower portion of the downstroke. Given the electromechanical delay, GM and Sol primarily contributed force to the pedal in the second half of Q2, across the bottom of the pedal cycle and through the first half of Q3, which explains the peak ineffective pedal force (away from the centre of crank rotation) occurring near the bottom dead centre of rotation (Figure 1).

2.4.3 Mechanical Power Output, Total Muscle Intensity, and Overall Efficiency

The MANCOVA showed that $\hat{I}_{PC4,LS}$ and $\hat{I}_{PC7,LS}$ were the most important covariates with η_O. The common features of $I_{PC4,W}$ and $I_{PC7,W}$ included changes to GM and the muscles acting across TDC (TA and RF) and the bottom of the pedal cycle (Sol, ST and BF). When η_O was at its maximum (55% and 60% O_{2max} trials) the ratio $I_{PC4,LS}$/$I_{PC1,LS}$ was only in its mid-range (Figure 3f), therefore η_O was very sensitive to $I_{PC4,LS}$/$I_{PC1,LS}$ with ratios too high or too low being associated with low η_O (90% and 25% O_{2max} conditions). It is possible that the coordination of muscle activity between left and right legs at the top and bottom of the cycle played an important role in η_O. Since the left and right crank arms are mechanically linked, the coordination patterns of a single leg and

22

the extrapolation to two legs may be insufficient to fully understand the influence of muscle coordination on η_O.

The reconstructed coordination patterns for high and low η_O highlight some of the differences in muscle activation (Figure 4). The coordination pattern for high η_O had a more even distribution of muscle activity across all muscles, whereas the coordination pattern for low η_O displayed large amounts of activity in GM, RF and to a lesser extent short bursts of VM and VL. At high η_O the intensities for the key power producing muscles, VM, VL and GM, were much more evenly distributed during the downstroke (Figure 4). Also, high η_O was associated with a regular progression of activity between the muscles; initially VM and VL synchronously, followed by GM, then Sol, then LG, MG, ST and BF synchronously. Conversely, with low η_O the muscle groups were activated less in concert (between VM and VL, and between LG, MG, ST and BF), and the EMG intensity of VL and GM were almost 90° apart. The timing of activation for GM and Sol was earlier at high η_O which, given the electromechanical delay, implies that these muscles provided force on the pedal for more of the power producing downstroke. Given the smooth and even distribution of EMG intensity and synchronization of peak muscle activity between muscles acting across the same joint, it is possible that the coordination pattern for high η_O results in smoother shifts from net knee joint moments to net hip joint moments that occur during the downstroke of the pedal cycle (van Ingen Schenau et al., 1992).

As the 90% O_{2max} condition was the most inefficient of all trials it had a large weighting on low η_O. Since GM had the largest range of activity between all conditions (Figure 2) it was a dominant feature of the 90% O_{2max} condition compared to the 55% and 60% O_{2max} trials, and this contributed to the differences in EMG intensity for GM between high and low η_O. When the pedal cycles from the 90% O_{2max} condition were excluded, there was still an uneven distribution of muscle activity in the reconstructed coordination patterns for low η_O with more weight on muscles acting on the ankle joint (TA, MG and LG) as well as RF and BF. Despite successful completion of the testing protocol by all participants, the 90% O_{2max} condition may have fatigued MG and LG (Bini et al., 2010; Dingwell et al., 2008), resulting in a greater reliance on GM and the knee extensor muscles to maintain the required power output. However, Bini and coworkers (2010) found that the mean ankle angle decreased with fatigue whereas in this study the mean ankle angle was reduced for higher η_O. This indicates that fatigue in

the ankle plantarflexors may not have been present or that the occurrence of fatigue in these muscles resulted in elevated efficiency when all muscles were considered, although this study did not investigate fatigue indicators of individual muscles across trials.

2.4.4 Methodological Considerations

The randomized block design was utilized to minimize bias on the EMG due to factors that are known to influence the signals such as muscle temperature and fatigue (De Luca, 1997). Lack of a significant difference between blocks for I_{tot} was evidence of successful implementation. When interpreting the coordination patterns, it is also important to account for the electromechanical delay. Assuming an electromechanical delay of 88 ms (van Ingen Schenau et al., 1992) the changes in muscle force would have occurred approximately 50º of pedal rotation after the EMG signal at a cadence of 95 rpm. The timing of the EMG relative to the pedal cycle is very sensitive to the pedal cadence because the electromechanical delay constitutes a larger proportion of the pedal cycle at higher cadences and so excitation is required earlier in the pedal cycle in order to apply force at a similar location in the cycle (Neptune et al., 1997). In this study there was no significant difference in cadence across conditions or blocks. However, similar to previous work, cadence was still a major source of variability and the PC that explained timing shifts (I_{PC2}) accounted for a substantial proportion of the muscle coordination patterns (Wakeling & Horn, 2009). $\hat{I}_{PC2,LS}$ was significantly correlated with cadence and by including it as a covariate in the MANCOVA the bias due to cadence was removed from the remaining results.

The results of this study rely on total EMG intensity from only ten leg muscles being an appropriate estimate of metabolic power and therefore energy consumption during cycling. Wakeling et al. (2011) used oxygen consumption to identify the relationship between metabolic power and total EMG intensity of ten leg muscles at workloads eliciting a respiration quotient above and below one (Figure 6). This means that metabolic power underestimated energy consumption since it did not consider anaerobic sources that become more significant at the highest workloads. This accounts for the non-linear relationship between metabolic power and total EMG intensity at the highest workloads found by Wakeling et al. (2011) and indicates that a linear relationship would exist if anaerobic energy was considered (Figure 6). It is important to note that this

study examines changes and differences in relative and not absolute values of efficiency. Therefore the overall mechanical efficiency used provides valuable insight into the relative muscle activity and energy costs of the mechanical work.

Figure 6.   Adapted from Wakeling et al. (2011). Relationship between metabolic power and total EMG intensity from 10 leg muscles during cycling.
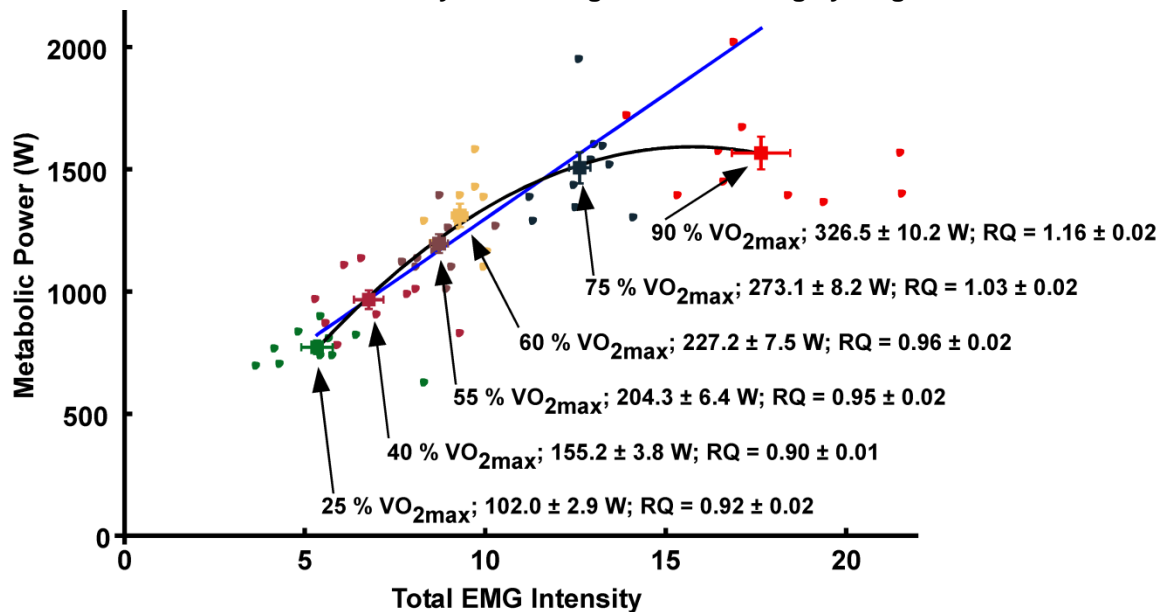
Squares show the mean ± SEM. for the ten subjects for each condition and a least squares 2nd order regression is fitted to the individual data points ($r^2 = 0.72$). Text shows the level of effort; mechanical power output; and the respiratory quotient, RQ, for each condition. Despite the non-linearity of the relationship at the highest workloads, there was a significant monotonic increase in metabolic power associated with increased EMG intensity (Spearman correlation, $r = 0.86$). Without the 90% O_{2max} condition there was improved correlation ($r = 0.91$) and the blue line shows a first order linear fit.

2.5 Conclusion

Significant relationships between muscle coordination patterns, power output, cadence, pedal forces, kinematics, I_{tot} and η_O were shown in this portion of the study. The highest η_O were not found at the highest power outputs and were dependent on the coordinated recruitment of all of the leg muscles examined. In particular high η_O was found at 55% to 60% O_{2max} with synchronized recruitment of muscles acting across the same joint and particular activation of muscles across the top and bottom of the pedal cycle. TA and RF appeared to play a vital role in maintaining increased ankle dorsi-flexion across TDC to allow for earlier application of force on the pedal at the beginning of the downstroke. While high η_O was dependent on the coordination of many muscles,

the highest power outputs were achieved primarily through increased GM and RF activity. The exchange of η_O for power output above and below 55% to 60% $\dot{V}O_{2max}$ implies there is a balance point where muscle coordination is optimal for efficient cycling.

CHAPTER 3: OUTDOOR STUDY

3.1 Introduction

Muscle activity in cycling has been well studied in the laboratory, yet there is a lack of research outdoors in a realistic cycling situation. It is important to conduct cycling research in a natural setting as conclusions and correlations from laboratory studies are limited by the ability to recreate realistic environmental conditions. For example, muscle activation research in cycling has primarily focused on the effects of progressively increasing or constant workloads on a limited number of muscles. This is in contrast to the reality of cycling where many muscles are active and workloads fluctuate according to the changing environment. This is a limitation of simulated time trial experiments where participants control the resistance, since changes in cadence and power output dictated by the environment are not considered. The purpose of this portion of the study was to determine the coordination patterns in time trial cycling outdoors and investigate their relationships to power output, I_{tot}, η_O, cadence, slope and distance.

3.2 Methods

3.2.1 Protocol and Data Acquisition

Nine competitive male cyclists cycled four laps of approximately 4.7 km each on paved roads in the shortest time possible. The participants gave their informed written consent to participate in the study in accordance with the Simon Fraser University Office of Research Ethics. Each lap of the course started and finished at the highest elevation and consisted of a descent followed by rolling and flat terrain before the final climb (Figure 7). The difference between the highest and lowest elevations was approximately 22 m. The participants were all tested at the same time of the morning within a three week period and wind and temperature measurements were taken at three different locations on the course for each participant.

Muscle activity of ten leg muscles (TA, MG, LG, Sol, VM, RF, VL, ST, BF and GM) was continuously recorded via surface EMG using Norotrode bipolar Ag/AgCl

Figure 7.   Elevation profile and map of a single lap in the outdoor cycling time trial.
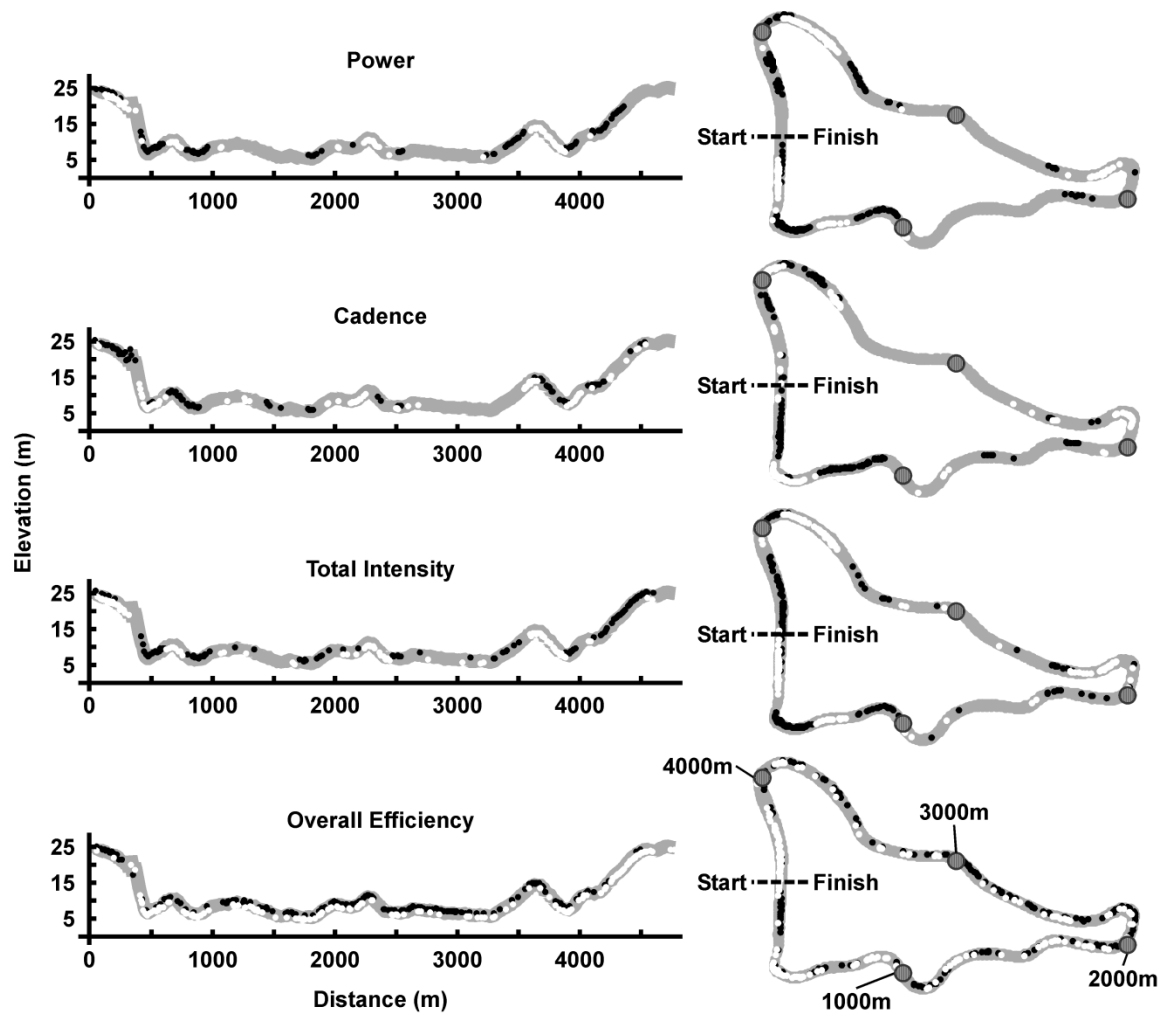
The 200 highest (black dots) and 200 lowest (white dots) pedal cycles ranked by cadence, power output, total EMG intensity and overall mechanical efficiency are shown on each figure.

surface electrodes (10 mm diameter, 21 mm interelectrode distance) (Myotronics, WA, USA). The signals were amplified (Biovision, Wehrheim, Germany) and sampled at 2000 Hz using a 16-bit analog to digital converter (USB-6210, National Instruments, Austin, USA) and LabVIEW software (National Instruments, Austin, USA). Unfortunately, due to the nature of outdoor data collection, there were many difficulties with noise and displacement of the EMG electrodes that could not be detected or fixed during the test. Consequently, data from three of the participants were eliminated as more than one muscle was missing a complete lap of data (six cyclists were analyzed: age 36.3 ± 3.0 years; mass 72.4 ± 2.0 kg; height 1.78 ± 0.18 m; distance cycled per year 9600 ± 2015 km; mean ± SEM.).

The participants cycled on their own racing bicycles equipped with SRM PowerControl and SRM PowerMeter crank arms (SRM, Schoberer Rad Meβtechnik, Jülich, Germany) that measured cycling data including power output, cadence and speed as well as heart rate through a Polar T31 transmitter (Polar Electro Oy, Finland). A global positioning system (GPS) (GPSmap 60CSx, Garmin International, Inc., KS, USA) was fastened to the cyclists to determine location, distance, speed and elevation profile throughout the test. The speeds recorded from the GPS and SRM units were used to synchronize the location, elevation and cycling data. In order to synchronize the EMG and cycling data, cadence was measured using both the SRM and a magnetic pedal switch, through the 16-bit analog to digital converter. The participants performed a 20-minute warm-up on their own bicycles mounted on a stationary cycle trainer (Cycleforce Swing, Tacx, Technische Industrie Tacx, Wassenaar, The Netherlands) prior to completing the time trial. They also used their own clipless pedals and were instructed to maintain a consistent position, seated with hands on the drop bars and pedal continuously for the duration of the trial.

3.2.2 Data Analysis

Mechanical power output was normalized to the mean of each participant due to the inter-subject variability in the measured values. The time-varying intensity of the EMG signals was calculated for each muscle (von Tscharner, 2000) and interpolated into 100 evenly spaced points for every pedal cycle such that the first point occurred when the pedal was at TDC. The interpolated EMG intensities for each muscle were normalized to its mean EMG intensity for the trial for each participant. Both I_{tot} and η_O were calculated on a pedal cycle by pedal cycle basis as in the indoor portion of this study (Chapter 2.2.2). Also, dominant muscle coordination patterns, including $I_{PC,W}$ and $I_{PC,LS}$ were identified for each pedal cycle using PC analysis on the EMG intensities from all muscles as described in the methods of the indoor potion of this study (Wakeling & Horn, 2009).

3.2.3 Statistics

With PC1 representing the dominant coordination pattern for all trails and all participants, the contribution of each $I_{PC,LS}$ relative to $I_{PC1,LS}$ for all pedal cycles was used in the analysis by normalizing each $I_{PC,LS}$ to $I_{PC1,LS}$ ($\hat{I}_{PC,LS}$). This implies that for a ratio of

one there was an equal amount of a particular $I_{PC,LS}$ to $I_{PC1,LS}$ even though the $I_{PC,W}$ may represent only a small percentage of the entire EMG signal. The coefficients for muscle coordination were statistically compared to the I_{tot}, mechanical power output, cadence, speed, heart rate, slope, η_O and distance using MANCOVA. I_{tot}, power output, cadence, slope, η_O and distance were tested individually as the dependent variable with subject as a random factor and the first 20 $I_{PC,LS}$s ($I_{PC1,LS}$ and $\hat{I}_{PC,LS}$ for all other PCs) as covariates using MANCOVA. Cadence was included as a covariate in each statistical analysis except where it was the dependent variable. Pairwise Pearson correlation coefficients were also determined for all factors and also included the total EMG intensity per muscle per pedal cycle. Statistical tests were considered significant at p≤0.05 and values are presented as mean ± SEM.

The sum of the vector products of the $I_{PC,W}$ and the $I_{PC,LS}$ ($\sum I_{PC,W}\,I_{PC,LS}$) reconstructs the instantaneous activation patterns for each pedal cycle. In order to visualize the effect of muscle coordination on each mechanical factor (power output, I_{tot} or η_O) the muscle coordination patterns were reconstructed using the first 20 PCs. If the $I_{PC,LS}$ had no significant effect on the mechanical factor then the mean $I_{PC,LS}$ from all pedal cycles was used in the reconstruction. If the $I_{PC,LS}$ had a significant effect on the mechanical factor then the pedal cycles were ranked by that factor, the top and bottom sets of 200 pedal cycles were extracted and the mean $I_{PC,LS}$ from each set was used in the reconstruction. The reconstructed patterns therefore highlight the primary features of muscle coordination for the highest and lowest of each mechanical factor. In addition, for η_O the muscle coordination patterns were reconstructed in a similar way for both the 200 pedal cycles with the highest normalized power outputs (100% group) and the 200 pedal cycles around the mean normalized power output (50% group; using 100 pedal cycles above and 100 pedal cycles below the mean).

3.3 Results

The mean cadence, power output and heart rate were 92.7 ± 0.5 rpm, 311.2 ± 2.5 W and 171.6 ± 0.4 bpm respectively and the mean power outputs for each lap were 326.6 ± 2.3 W, 311.0 ± 1.3 W, 300.9 ± 1.2 W and 305.4 ± 1.6 W for laps 1, 2, 3 and 4 respectively. The wind speed was less than five km/h for all measurements and the mean temperature was 21.7 ± 0.7 °C. The participants each traveled 18,683.4 ± 28.7 m during the time trial depending on the line of travel on the road.

3.3.1 Muscle Activation

The first ten PCs explained over 79% of the EMG signal with the first PC explaining over 52%. The first PC can be visualized through the $I_{PC1,W}$ (Figure 8) and was highlighted by heightened peak activation of VL and RF. $I_{PC2,W}$ differentiated between activation in VL and RF and activation in all other muscles, most notably MG and LG, and $I_{PC3,W}$ uncoupled VL and RF (Figure 8). Both $I_{PC1,LS}$ and $\hat{I}_{PC2,LS}$ were significantly correlated with power output and I_{tot} (r=0.69 and 0.97 for $I_{PC1,LS}$ and r=0.51 and 0.68 $\hat{I}_{PC2,LS}$ respectively; Figure 9) and all three knee extensor muscles monitored (VL, VM and RF) and Sol were significantly positively correlated with both $I_{PC1,LS}$ and $\hat{I}_{PC2,LS}$ (r=0.77, 0.78, 0.83 and 0.72 for $I_{PC1,LS}$ and r=0.69, 0.58, 0.68 and 0.50 for $\hat{I}_{PC2,LS}$ respectively).

Mean total EMG intensity per pedal cycle and timing differences for the individual muscles were observed between laps. There was a general decrease from lap 1 to lap 4 in the mean total EMG intensity per pedal cycle for ST, BF, VL, RF and TA (Figure 10); in contrast there was a general increase for Sol and GM. The mean coordination patterns for each lap were similar in timing, but differed in amplitude with lap 1 demonstrating emphasized VL activation, laps 2 and 3 showing increased peak MG and LG activation and lap 4 having elevated peak RF, VM, Sol, MG and LG activity (Figure 11). A shift in timing for most muscles was revealed in $I_{PC4,W}$ and $\hat{I}_{PC4,LS}$ and was significantly correlated with heart rate (r=0.60).

3.3.2 Mechanical Power Output

There was a significant correlation between power output and I_{tot} (r=0.74; Figure 9) with eight of the first twenty PC loading scores significantly related to power output. The high power output pedal cycles used in the reconstructed signal had a large contribution of VL and RF relative to the other muscles whereas the lower power output cycles had a larger relative contribution of MG and LG (Figure 12). Additionally, aside from an overall increase in I_{tot}, the reconstructed patterns for the highest power outputs revealed more EMG intensity prior to and at TDC for TA, VM, RF and VL, and later activation of Sol, ST, BF and GM at the bottom and first part of the upstroke when compared to the lowest power outputs (Figure 12). At high power outputs the peak activation of most muscles occurred within three synchronized groups: the knee extensors, followed by Sol, GM and BF, and finally MG, LG and ST. In contrast the low

Figure 8.   Principal component weightings for the EMG intensities during the outdoor trial.
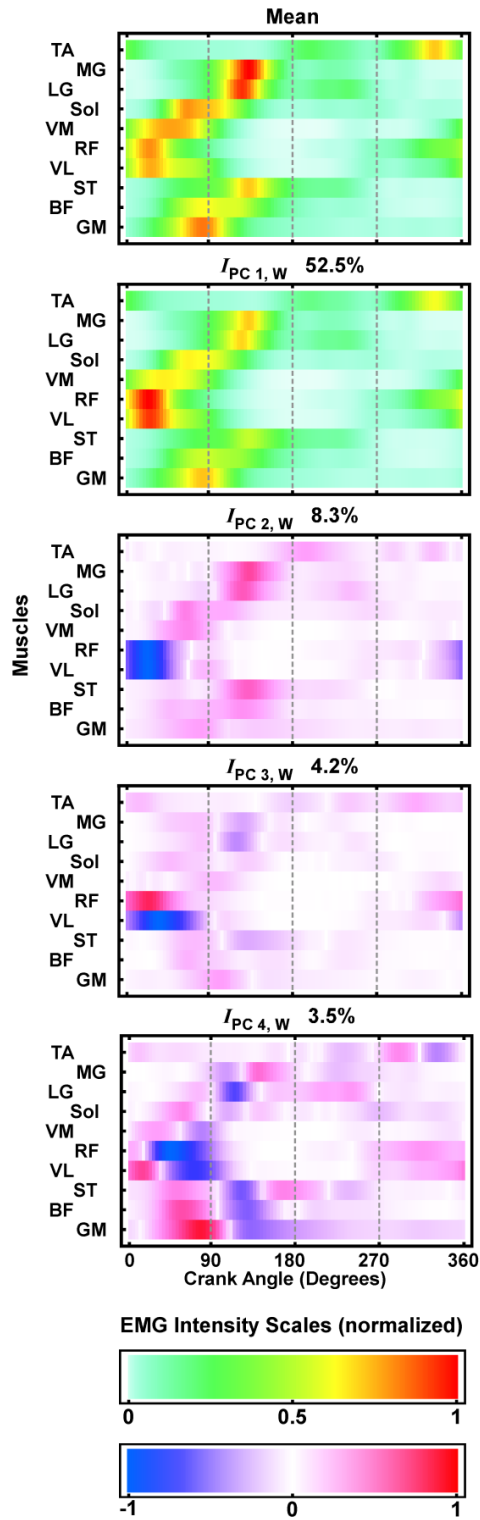
The first row represents the mean EMG intensity and subsequent rows are representations of the first four PC weightings (PC, W) showing the percentage of the data set explained by each PC, W. Figure scales are shown at the bottom.

Figure 9. Relationships between power output, total EMG intensity, overall mechanical efficiency (power output/ total EMG intensity), slope, cadence and the principal component loading scores (The $\hat{I}_{PC2,\,LS}$ (d, e and f) represents the ratio of $I_{PC2,\,LS}$ to $I_{PC1,\,LS}$.).
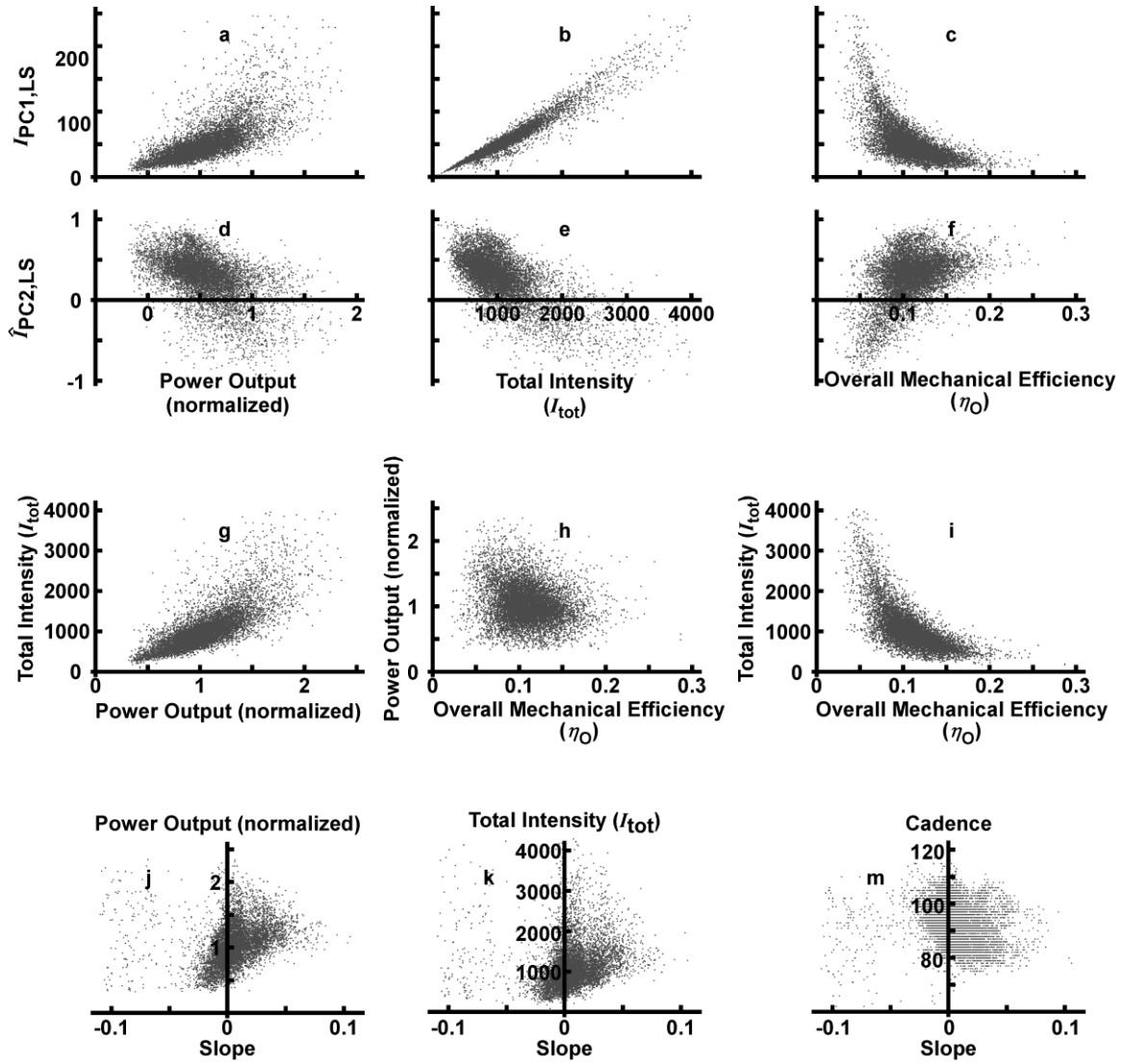
Figure 10. Mean total EMG intensity per pedal cycle per lap for each muscle (TA, MG, LG, Sol, VM, RF, VL, ST, BF and GM) for the outdoor time trial. Values are presented as mean ± SEM.
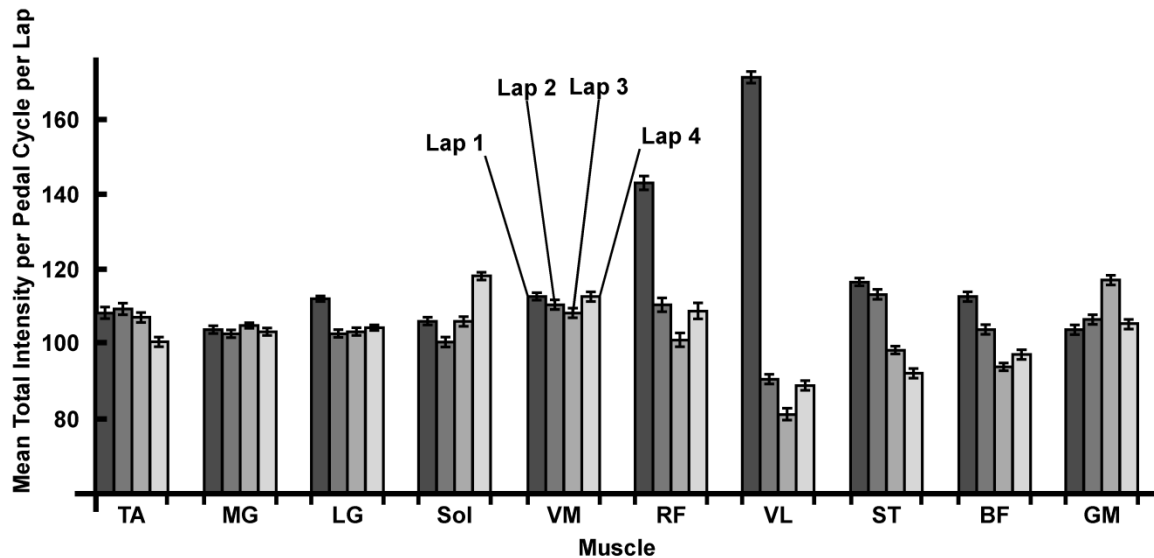
power outputs showed variation in the timing of peak activation within these three groups of muscles (Figure 12). Of the high power output pedal cycles, 106 occurred between the start and 1000 m, 65 per 1000 m occurred between 4000 m and the start-finish line (since the distance between 4000 m and the finish line was less than 1000 m the value per 1000 m has been used for comparison) while only 46 occurred between 1000 m and 4000 m (Figure 7).

3.3.3 Slope

Slope demonstrated significant positive and negative relationships with power output and cadence respectively (Figure 9) and seven of the first twenty PC loading scores were significantly related to slope. Reconstructed EMG traces at high slopes showed increased GM activity during the downstroke, earlier peak activation of BF and VM, later and increased peak activation of RF and decreased peak activation of TA and ST. Also, there was a more even distribution of activation between the knee extensors, ankle extensors and GM for high slopes whereas lower slopes were more dependent on MG and LG. The mean normalized power outputs for high and low slopes were 1.260 ± 0.014 and 1.13 ± 0.04 with non-normalized power outputs of 369.5 ± 4.1 W and 330.5 ± 11.2 W respectively.

Figure 11. **Mean EMG intensity for each muscle (TA, MG, LG, Sol, VM, RF, VL, ST, BF and GM) for each lap of the outdoor time trial.**
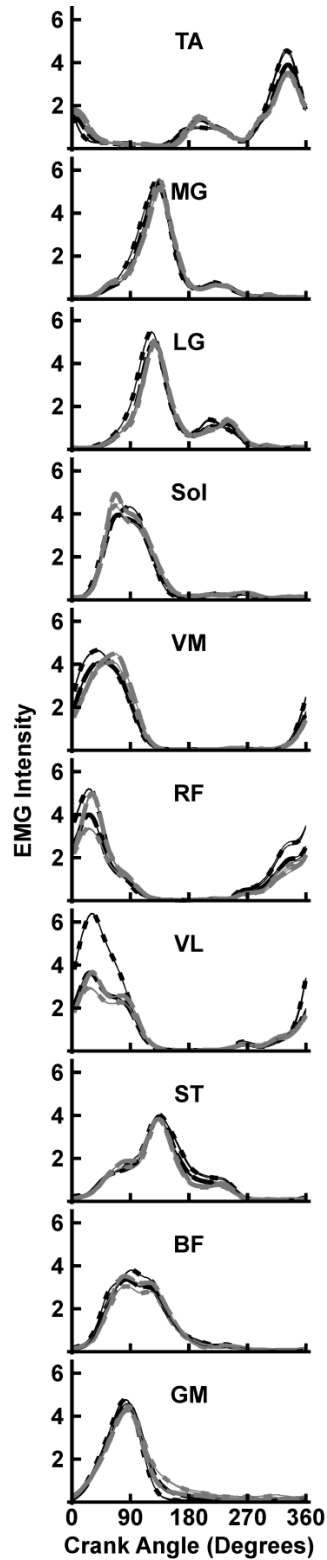
Lap 1 (black short dashed line), lap 2 (black long dashed line), lap 3 (grey short dashed line) and lap 4 (grey long dashed line) are shown with mean ± SEM (solid lines for all laps).

Figure 12. Outdoor coordination patterns reconstructed from the PC analysis for all muscles with respect to power output.
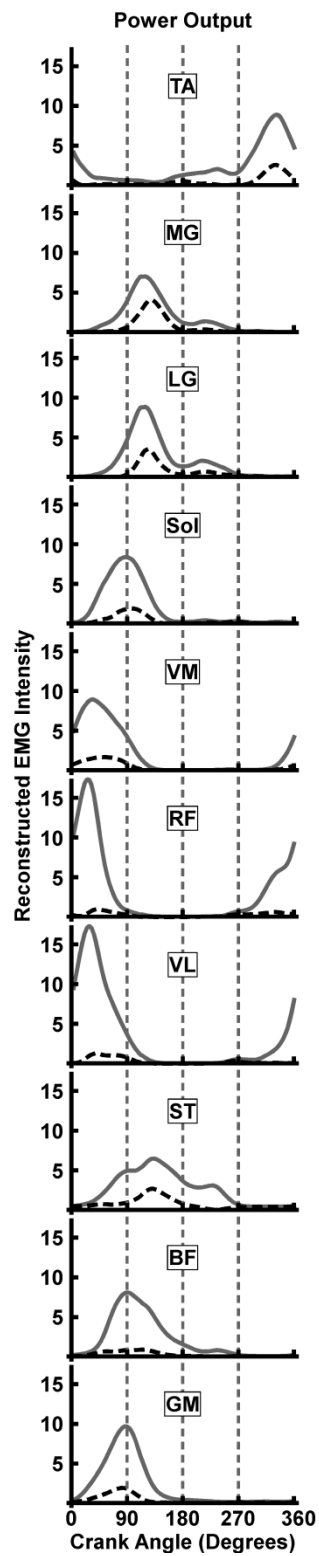
The patterns are reconstructed with respect to high (grey line) and low (black dashed line) power output. The first twenty PCs were used for the reconstruction.

3.3.4 Overall Mechanical Efficiency

There was a significant negative correlation between η_O and I_{tot} (r=-0.69; Figure 9), a significant positive correlation between I_{tot} and power output (r=0.74; Figure 9) and no significant relationship between η_O and power output (Figure 9). Twelve of the first twenty PC loading scores showed significant relationships to η_O and η_O had significant negative relationships with $I_{PC1,LS}$ and $\hat{I}_{PC2,LS}$ (r=-0.65 and -0.45 respectively; Figure 9). As $I_{PC2,W}$ separated RF and VL from the other muscles monitored, at high η_O there was less RF and VL relative to the other muscles, which was reversed for low η_O pedal cycles. Changes to RF, VL and TA across TDC, GM and Sol at 25% of the pedal cycle and ST and BF during the downstroke and across the bottom of the pedal cycle were the primary features of the PCs showing significant relationships to η_O. Reconstructed signals for high and low η_O showed large amounts of EMG intensity for RF and VL relative to the other muscles for low η_O (Figure 13). The emphasis was shifted from RF and VL to the MG and LG for high η_O (Figure 13).

Examination of the reconstructed coordination patterns for high and low η_O at similar power outputs revealed power output dependent differences despite no significant relationship between power output and η_O. The relative contribution of RF and VL to increased I_{tot} (η_O = mechanical power output/ I_{tot}) was reduced at 50% compared to 100% power output. At 100% power output there were large spikes of EMG intensity for RF, VL and TA relative to all other muscles for the low η_O (Figure 13). Also at 100% power output the activation of ST, MG and LG was similar for high and low η_O while all other muscles had higher EMG intensity amplitudes for low η_O. There was an even distribution of peak activation at 100% power output among most muscles for high η_O that was not as apparent for low η_O. At 50% power output there was more muscle activity during the upstroke, particularly in TA, LG, RF and VL for low η_O. The mean normalized power outputs for the high and low η_O groups were 1.548 ± 0.003 and 1.544 ± 0.003 respectively for 50% power output and 1.922 ± 0.015 and 1.942 ± 0.019 respectively for 100% power output. The pedal cycles for both high and low η_O occurred at similar locations on the course for both 50% and 100% power outputs.

3.4 Discussion

The main findings of this study provide evidence that muscle coordination, power output and overall mechanical efficiency are dependent on the distribution of power and

Figure 13. Outdoor coordination patterns reconstructed from the PC analysis for the TA, MG, LG, Sol, VM, RF, VL, ST, BF and GM with respect to mechanical efficiency.
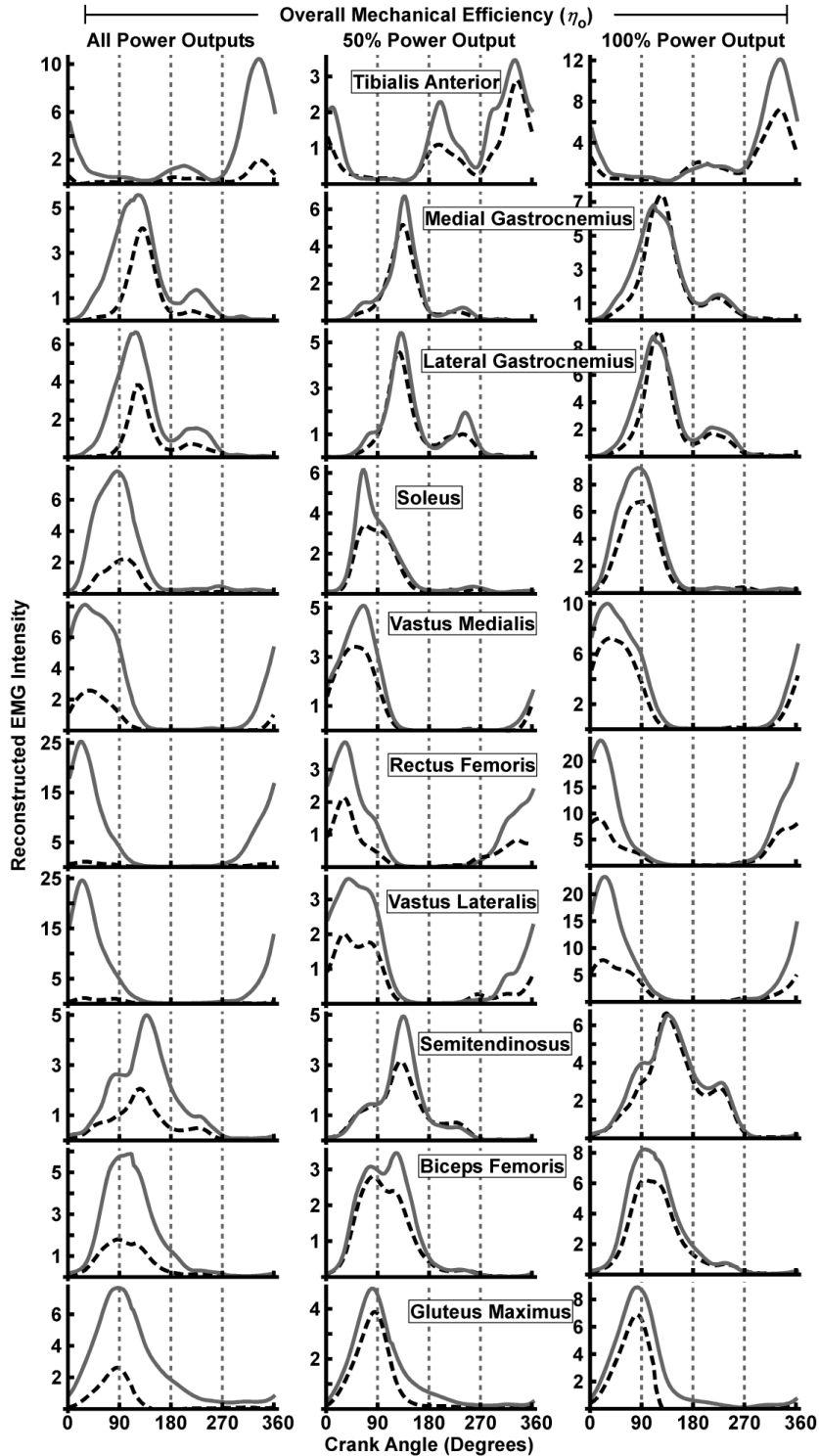
The patterns show high (solid grey line) and low (black dashed line) states of overall mechanical efficiency, using all pedal cycles (first column), 100 pedal cycles above and below 50% power output (second column) and 200 pedal cycles at 100% power output (third column). The first twenty PCs were used for each reconstruction.

the terrain profile in outdoor cycling time trials. Also, overall mechanical efficiency depends on the coordination of multiple muscles, particularly synchronized activation of muscles acting across the same joint and those active at the top and bottom of the pedal cycle, and not just the primary power producers during an outdoor cycling time trial. Similarly, high power output is dependent on coordinated recruitment of muscles acting across the same joint and elevated activation of RF and VL.

3.4.1 Indoor and Outdoor Cycling

The mean cadence was similar to values found in male multi-stage cycling races (Lucia et al., 2001). The standard deviation was 7.9 rpm and is indicative of the variance in cadence utilized by different participants in variable terrain. With cadence normalized to each participant, there was still a significant negative relationship between cadence and slope suggesting the deviation in cadence was in part due to variations in slope. This is not surprising since cyclists use lower cadences in hilly and mountainous stages in male cycling races (Lucia et al., 2001).

The timing and duration of muscle activation in both $I_{\text{PC1,W}}$ and the mean coordination pattern were similar, but not identical to those found in indoor studies such as Wakeling and Horn (2009) (Figure 8). It is not unexpected that they differ considering coordination patterns change with cadence and resistance (Hug & Dorel, 2009; Wakeling & Horn, 2009). The closest cadence matched condition used by Wakeling and Horn (2009) was 100 rpm with a resistance equivalent to approximately 70 W which was comparable in timing for most muscles except GM. This is understandable given that 70 W is considerably lower than the mean power output in this study and GM activity is dependent on resistance and not highly active at low power outputs (Ericson et al., 1985). The closest power matched condition had a resistance of approximately 250 W where GM activation was closer to our study, but the cadence was far lower at only 60 rpm. This resulted in earlier peak VM and VL activity which was also found at higher slopes in this outdoor trial where cadences were lower. This provides further evidence that disparities in muscle coordination can be explained by the differences in cadence and resistance (Hug & Dorel, 2009). These fluctuations in cadence and resistance resulting in altered power output and muscle coordination occur naturally on outdoor terrain, but are more difficult to simulate indoors on a stationary bicycle.

3.4.2 Power Output and Muscle Activity

Similar to indoor studies, increased power outputs or workloads were associated with increased levels of muscle activity as shown by the significant positive relationships between power output and both I_{tot} and $I_{PC1,LS}$ (Bini et al., 2008; Ericson et al., 1985; Macdonald et al., 2008; St Clair Gibson et al., 2001). Although all muscles displayed positive EMG intensities in $I_{PC1,W}$, RF and VL were the muscles most responsible for higher power outputs since these were the only muscles showing positive increases in $\hat{I}_{PC2,LS}$ with rising power outputs. This adds evidence that VL is a primary power producing muscle in cycling (Ryan & Gregor, 1992) and that RF and power output have a positive relationship in time trial cycling (Bini et al., 2008; St Clair Gibson et al., 2001) both indoors and outdoors.

Along with increased I_{tot}, there was more synchronized activation of the muscles acting across the same joint at high power outputs. During the downstroke in cycling peak joint moments occur in sequence from knee to hip to ankle (van Ingen Schenau et al., 1992) and a similar progression occurred in this study for muscle activation. The knee extensors were active synchronously followed by GM, BF and Sol and then MG, LG and ST (Figure 12). The Sol is known to be more active at higher resistances than MG and LG (Wakeling & Horn, 2009) and at a similar location in the pedal cycle to GM to stabilize the ankle to transfer power to the pedal (Neptune et al., 2000; Ryan & Gregor, 1992). Also ST, MG and LG are bi-articulate muscles which can transfer power between the joints (van Ingen Schenau et al., 1992), therefore they may have acted to transfer the joint moments from the hip to the ankle. The highly synchronized muscle activation transferred between joints at high power outputs is not unexpected given that increasing power outputs have previously been shown to be dependent on muscle coordination (Wakeling et al., 2010).

3.4.3 Muscle Coordination, Power Output and Overall Mechanical Efficiency Dependent on Pacing and Slope

The significant relationships between the PCs, power output, η_O and slope show that muscle coordination, power output and η_O fluctuate during an outdoor time trial and that the fluctuations are partially dependent on the slope. Similar to male cycling races, there was an increasing relationship between power output and slope (Padilla et al., 2001; Vogt et al., 2006). The higher power outputs occurred on the uphill sections of the

course when the cadences were the lowest. Visually this can be seen in Figure 7 where the majority of the highest power output pedal cycles occurred on uphill sections of the course. The lower cadences contribute power to more of the downstroke by allowing for earlier onset of power production at the start of the pedal cycle and longer duration of activation. This can be seen through the reconstructed coordination patterns for high and low power output which showed increased TA, VM, RF and VL at TDC and early in the pedal cycle and more Sol, ST, BF and GM activity later in the downstroke (Figure 12). This is similar to the high resistance, low cadence trial in the Wakeling and Horn (2009) study where peak knee extensor activation was very close to TDC with heightened activation continuing early in the pedal cycle and more Sol, ST and GM activity in the latter portion of the downstroke.

VL and RF followed the same trend in activation as the pacing strategy utilized in the outdoor time trial with both the mean power output per lap and VL and RF EMG intensities resembling a reverse J-shaped pacing strategy (Figure 10; (Abbiss & Laursen, 2008)). This is similar to previous findings showing significant increases in VL activity throughout a 40 km time trial (Bini et al., 2008), no change in RF during a 30 minute time trial (Duc et al., 2005) and decreased RF through a 100 km time trial (St Clair Gibson et al., 2001). It should be noted that the 40 km time trial used negative pacing (Bini et al., 2008), the 30 minute time trial used even pacing (Duc et al., 2005) and the 100 km time trial had positive pacing (St Clair Gibson et al., 2001). The 40 km time trial showed no change in RF activity which is partly explained by the environmental conditions (Bini et al., 2008). Lower cadences and increased RF at TDC would not be found in indoor studies using a constant cadence such as the 40 km time trial since these outcomes were found on higher slopes in this outdoor study.

Of the pedal cycles with the highest η_O, the largest concentrations were located on the slight downhill sections and the transitions from uphill to downhill with few occurring on the longest uphill section at the end of each lap (Figure 7). In contrast, the largest concentrations of pedal cycles with the lowest η_O were located in the transitions from downhill to uphill and on the uphill sections (Figure 7). This implies that at high intensities of outdoor time trial cycling η_O is maximized where the resistance due to slope is decreasing and minimized where it is increasing. Subsequent retrospective analysis did not identify a significant relationship between acceleration and η_O although with the

continuous changes in acceleration on undulating terrain it may be too difficult to detect such a relationship.

3.4.4 Fluctuations in Muscle Activity Mitigate Muscle Fatigue

The fluctuations in muscle activity that resulted from the course profile may mitigate muscle fatigue that has previously been reported from more controlled indoor cycling trials (Housh et al., 2000; Petrofsky, 1979) since there were no significant relationships between the muscle coordination patterns and distance. An effect of distance (or time) on muscle coordination would be expected if fatigue had progressed over the duration of the time trial as occurred in indoor cycling studies displaying muscle fatigue (Housh et al., 2000; Petrofsky, 1979). Similar to other indoor time trial studies, typical fatigue indices, such as increased muscle activation, were not observed for most muscles in this study (Bini et al., 2008; Duc et al., 2005). Additionally, the muscles known to be susceptible to fatigue such as MG and LG (Bini et al., 2010; Dingwell et al., 2008) had stable EMG intensities for each lap (no significant difference in mean lap EMG intensity except MG lap 1, which was significantly higher; Figure 10). Duc (2005) suggested that time trials do not induce significant quadriceps fatigue in competitive cyclists, which was supported in our study. The ability of the cyclists to self-regulate the pacing was a commonality between the indoor time trial studies by Bini et al. (2008) and Duc et al. (2005) and this study, which was not applicable to greater-controlled indoor trials displaying muscle fatigue (Housh et al., 2000; Petrofsky, 1979). Cyclists in the Bini et al. (2008) and Duc et al. (2005) indoor time trials regulated their pacing by adjusting the resistance, whereas fluctuating terrain also influenced resistance in the present study. The shifting activation between each muscle may have provided adequate rest to avoid performance-reducing fatigue and maintain power output for the duration of the time trial as postulated by St Clair Gibson (2001). Whether dictated by terrain or self-adjusted, this implies that variable resistance diminishes the potential for fatigue during a time trial.

3.4.5 Overall Mechanical Efficiency and Mechanical Power Output

High η_O occurred at power outputs lower than the maximum and may depend on specific muscle activation timing around the top and bottom of the pedal cycle and activation in more than just the knee extensor muscles. The transition from upstroke to

downstroke (across TDC of the pedal cycle) seems to be important to producing power early in the pedal cycle, thereby maximizing the power output with minimal muscle activation in time trial cycling. Some of the key changes in TA, RF, VL, ST and BF EMG intensities related to η_O occurred at the transitions between the downstroke and upstroke (across top and bottom dead centre of the pedal cycle) when little force is applied perpendicular to the crank arms in cycling (Patterson & Moreno, 1990; Patterson et al., 1983; Sanderson, 1991). Coordinated recruitment between the muscles of the left and right legs could be the most important factor because of the mechanical link between the crank arms. The pedal cycle would be disrupted if there were resistive forces from the opposite pedal through the transitions since the effective forces are small. This is not a problem where forces are highest during the downstroke as some cyclists exhibit relatively small resistive forces during the upstroke while power output remains stable (Patterson & Moreno, 1990; Patterson et al., 1983; Sanderson, 1991). Regardless of the specific explanations, these transitions appear to play a key role in η_O despite minimal forces acting on the pedals.

The reconstructed signals for high and low η_O for all pedal cycles was dependent on the interplay between RF and VL activity and MG and LG activity, as shown in the reconstructed coordination patterns (Figure 13) and the negative relationship between η_O and $\hat{I}_{PC2,LS}$ (Figure 9). Contrary to RF and VL, VM had little influence on η_O. The amount of vastii activation differed considerably depending on the resistance despite being thought of as a primary power producing muscle and showing very consistent activation timing previously (Ryan & Gregor, 1992). Ericson (1985) evaluated only VM at different power outputs showing consistency with minimal change in muscle activity. VM may be consistently active regardless of the power output, while VL fluctuates with power and is therefore more involved at the higher power outputs associated with time trial intensities. This would not be unexpected as VL followed the pacing strategy and changed with power output in this study and in the simulated indoor time trial of Bini et al. (2008).

Despite no significant relationship between power output and η_O, the power outputs for high and low η_O were substantially different: 0.96 ± 0.02 and 1.21 ± 0.03 normalized power output respectively. Examination of η_O at 50% and 100% of the maximum power output were used to minimize the influence of power output on the reconstructed coordination patterns since muscle coordination changes with power output. At 100% power output, high and low η_O were associated with altered RF and VL

activity, whereas at 50% the changes in η_O were due to other muscles (Figure 13). Activation of many muscles to produce high power outputs was more efficient than relying solely on the knee extensors since high η_O for 100% power output displayed an even distribution of peak activation among most muscles. When power outputs were not as high in the 50% power pedal cycles, η_O was dependent on minimizing muscle activation during the upstroke.

3.4.6 Methodological Considerations

There are many difficulties when conducting muscle activation studies in an outdoor environment as compared to an indoor laboratory setting. Most notably are variables such as equipment, weather and terrain. To record EMG signals continuously for 30 minutes at 2000 Hz requires a reliable portable power source, large amounts of portable data storage and consistent contact between the electrodes and the skin. Unfortunately due to adhesion problems, that are normally detected and corrected real-time in the laboratory, three of the participants' data had to be excluded from the analysis. To minimize the effects of weather on the study the participants were all tested at the same time of day, since both wind resistance (Davies, 1980) and temperature (Tatterson et al., 2000) are factors known to affect cycling performance. Wind and temperature measurements were taken at three different locations on the course for each participant and the conditions were similar with wind speeds less than five km/h and mean temperature of 21.7 ± 0.7 °C over the three week testing period.

Dorel (2009) showed increased GM activity in an aerodynamic position compared to riding with hands on the drop bars. Cyclists were instructed to ride with their hands on the drop bars, but they could have adopted a more aerodynamic position by reducing the hip joint angle due to air resistance. Future outdoor studies should include joint angles to help control for the influence of altered body position on muscle coordination.

As previously discussed in the indoor portion of this study, the estimate of overall mechanical efficiency relies on the relationship between total EMG intensity and energy consumption. The time trial was over 18 km long and the mean power output was over 300 W. This indicates that the participants were cycling between 75 and 90% $\dot{V}O_{2max}$ based on the indoor study results since the participants of the indoor and outdoor studies had similar characteristics and training backgrounds with some subjects

completing both portions of the study. Again, Wakeling et al. (2011) found a significant relationship between metabolic power and total EMG intensity (Figure 6) that was non-linear at the highest workloads. When considering all workloads except 90% $\dot{V}O_{2max}$ there was a significant linear relationship between metabolic power and total EMG intensity (r^2=0.79; correlation r=0.89) that is an improvement on the 2nd order fit found by Wakeling et al. (2011). This indicates that using total EMG intensity as a proxy for energy consumption at respiration quotients above one is not a problem considering the linear relationship includes the 75% $\dot{V}O_{2max}$ trial with a respiration quotient above one. Therefore this study provides useful information about relative overall mechanical efficiency despite the significant role of anaerobic energy sources utilized during the cycling time trial when efficiency was derived using only aerobic sources.

CHAPTER 4: CONCLUSION

In support of the hypotheses, this study shows that there are significant relationships between muscle coordination, forces acting on the pedals, mechanical power output, I_{tot}, kinematics and η_O in both indoor and outdoor cycling. It does not compare indoor to outdoor cycling directly, but provides evidence that muscle activity, power output and η_O are dependent on the measurement conditions.

While there was a significant positive correlation between power output and I_{tot} indoors and outdoors, the muscles demonstrating the largest changes in EMG intensity differed. RF and GM showed the largest increases with power output indoors with VM and VL consistently active. In the outdoor portion of the study RF and VL displayed the most pronounced positive relationships with power output while VM was consistently active. This is both supportive and contrary to the hypothesis that greater vastii activation would occur at higher power outputs since VM was consistently active both indoors and outdoors and VL was consistently active indoors while displaying increased activity with power output outdoors. An explanation why GM was a larger source of variability than VL during the indoor trial is that VL varies with the relatively small fluctuations in power output during simulated time trials (Bini et al., 2008), whereas GM shows a large range of activation from low to high power outputs (Ericson, 1986) as was present during the indoor study. VM, VL and GM have previously been reported as primary power producing muscles in cycling (Ericson, 1986; Ryan & Gregor, 1992); this study adds RF as a consistently important muscle for increased power production in both indoor and outdoor cycling.

In a previous study, coordinated muscle recruitment was a key factor in determining the mechanical efficiency of limb movement (Wakeling et al., 2010). Similarly, this study demonstrates that η_O in both indoor and outdoor cycling is dependent on the activation levels, timing and coordination of the all of the active leg muscles and not any one muscle in particular, which supports the hypothesis that η_O would be significantly associated with muscle coordination. Although η_O was related to muscle coordination it was independent of the direction of applied pedal force, yet could be seen through the changes in the amplitude of the force. This was contrary to the

46

hypothesis that pedal effectiveness would be significantly associated with muscle coordination patterns, but supports another study demonstrating that large variations in muscle activity are not matched by similar variations in pedal force application (Hug et al., 2008). Additionally, this study shows that there exists a trade-off between power and efficiency in cycling since the highest mechanical efficiencies did not occur at the highest power outputs. Increased η_O was achieved through coordinated contraction of muscles acting across the same joint, such as VL and VM, peak muscle activity occurring sequentially from knee to hip to ankle, and the reliance on multiple muscles to produce large joint torques. Given that both left and right legs are used for cycling and the crank arms are not independent, coordinated recruitment between the muscles of the left and right legs could play an important role in efficient cycling. The most striking evidence of this was the significant relationship between η_O and the variability in coordination of muscles across the top and bottom of the pedal cycle. Future muscle coordination studies in cycling should include the coordination between both legs due to the mechanical dependence of the crank system.

In practical terms this study may have implications on training techniques for cycling. Training in specific conditions would maximize the use of muscle coordination patterns realized in competition given that the coordination patterns vary with resistance which changes with workload and terrain. For example the trade-off between power output and overall efficiency indicates that short sprint cycling events that require high power outputs would sacrifice efficiency for power output. These cyclists would benefit from training as much as possible at these high power outputs to maximize their exposure to the corresponding muscle coordination patterns. Cycling to maximize overall efficiency at 55-60% O_{2max} or cycling at lower resistances would promote a different set of muscle coordination patterns which would emphasize and strengthen different muscles. These coordination patterns would be more suited to multi-stage cycling races where overall efficiency is more important. Although if long climbs during the multi-stage races are the most important factor, training on these slopes would maximize the coordination patterns resulting from lower cadence and higher power output that occur at steeper slopes. In reference to scientific studies, since the coordination patterns vary with resistance and cadence, deductions from laboratory studies should be cautious in interpretations outside the bounds of their specific conditions. Therefore this study highlights the importance of measuring in the field or at least careful reproduction of outdoor environments in indoor studies.

REFERENCE LIST

Abbiss, C. R., & Laursen, P. B. (2008). Describing and understanding pacing strategies during athletic competition. *Sports Med.*, *38*(3), 239–252.

Arnaud, S., Zattara-Hartmann, M. C., Tomei, C., & Jammes, Y. (1997). Correlation between muscle metabolism and changes in M-wave and surface electromyogram: dynamic constant load leg exercise in untrained subjects. *Muscle Nerve.*, *20*(9), 1197-1199.

Bigland-Ritchie, B., & Woods, J. J. (1976). Integrated electromyogram and oxygen uptake during positive and negative work. *J Physiol.*, *260*(2), 267–277.

Bini, R. R, Diefenthaeler, F., & Mota, C. B. (2010). Fatigue effects on the coordinative pattern during cycling: Kinetics and kinematics evaluation. *J Electromyogr Kinesiol.*, *20*(1), 102-107.

Bini, R. R., Carpes, F. P., Diefenthaeler, F., Mota, C. B., & Guimaraes, A. C. S. (2008). Physiological and electromyographic responses during 40-km cycling time trial: relationship to muscle coordination and performance. *J Sci Med Sport.*, *11*(4), 363-370.

Chapman, A. R., Vicenzino, B., Blanch, P., & Hodges, P. W. (2008). Patterns of leg muscle recruitment vary between novice and highly trained cyclists. *J Electromyogr Kinesiol.*, *18*(3), 359–371.

Coyle, E. F., Feltner, M. E., & Kautz, S. A. (1991). Physiological and biomechanical factors associated with elite endurance cycling performance. *Med Sci Sports Exerc.*, *23*(1), 93-107.

Davies, C. T. M. (1980). Effect of air resistance on the metabolic cost and performance of cycling. *Eur J Appl Physiol O.*, *45*(2-3), 245.

De Luca, C. J. (1997). The use of surface electromyography in biomechanics. *J Appl Biomech.*, *13*(2), 135–163.

Dingwell, J. B., Joubert, J. E., Diefenthaeler, F., & Trinity, J. D. (2008). Changes in muscle activity and kinematics of highly trained cyclists during fatigue. *IEEE Trans Biomed Eng.*, *55*(11), 2666-2674.

Dorel, S., Couturier, A., & Hug, F. (2008). Intra-session repeatability of lower limb muscles activation pattern during pedaling. *J Electromyogr Kinesiol.*, *18*(5), 857–865.

Dorel, S., Couturier, A., & Hug, F. (2009). Influence of different racing positions on mechanical and electromyographic patterns during pedalling. *Scand J Med Sci Sports.*, *19*(1), 44-54.

Dorel, S., Drouet, J. M., Couturier, A., Champoux, Y., & Hug, F. (2009). Changes of pedaling technique and muscle coordination during an exhaustive exercise. *Med Sci Sports Exerc.*, *41*(6), 1277-1286.

Duc, S., Betik, A. C., & Grappe, F. (2005). EMG activity does not change during a time trial in competitive cyclists. *Int J Sports Med.*, *26*(2), 145–150.

Ericson, M. O. (1986). On the biomechanics of cycling. A study of joint and muscle load during exercise on the bicycle ergometer. *Scand J Rehabil Med Suppl.*, *16*, 1-43.

Ericson, M. O., Nisell, R., Arborelius, U. P., & Ekholm, J. (1985). Muscular activity during ergometer cycling. *Scand J Rehabil Med.*, *17*(2), 53-61.

Hettinga, F. J., De Koning, J. J., Broersen, F. T., Van Geffen, P., & Foster, C. (2006). Pacing strategy and the occurrence of fatigue in 4000-m cycling time trials. *Med Sci Sports Exerc.*, *38*(8), 1484-1491.

Housh, T. J., Perry, S. R., Bull, A. J., Johnson, G. O., Ebersole, K. T., Housh, D. J., & devries, H. A. (2000). Mechanomyographic and electromyographic responses during submaximal cycle ergometry. *Eur J Appl Physiol.*, *83*(4), 381–387.

Hug, F., Bendahan, D., Le Fur, Y., Cozzone, P. J., & Grelot, L. (2004). Heterogeneity of muscle recruitment pattern during pedaling in professional road cyclists: a magnetic resonance imaging and electromyography study. *Eur J Appl Physiol.*, *92*(3), 334–342.

Hug, F., & Dorel, S. (2009). Electromyographic analysis of pedaling: a review. *J Electromyogr Kinesiol.*, *19*(2), 182–198.

Hug, F., Drouet, J. M., Champoux, Y., Couturier, A., & Dorel, S. (2008). Interindividual variability of electromyographic patterns and pedal force profiles in trained cyclists. *Eur J Appl Physiol.*, *104*(4), 667–678.

Jammes, Y., Arbogast, S., Faucher, M., Montmayeur, A., Tagliarini, F., & Robinet, C. (2001). Interindividual variability of surface EMG changes during cycling exercise in healthy humans. *Clin Physiol.*, *21*(5), 556–560.

Johnson, M. A., Polgar, J., Weightman, D., & Appleton, D. (1973). Data on the distribution of fibre types in thirty-six human muscles: An autopsy study. *J Neurol Sci.*, *18*(1), 111-129.

Kautz, S. A., Feltner, M. E., Coyle, E. F., & Baylor, A. M. (1991). The pedaling technique of elite endurance cyclists: changes with increasing workload at constant cadence. *J Appl Biomech.*, *7*(1), 29-53.

Li, L. (2004). Neuromuscular control and coordination during cycling. *Res Q Exerc Sport.*, *75*(1), 16-22.

Lucia, A., Hoyos, J., & Chicharro, J. L. (2001). Preferred pedalling cadence in professional cycling. *Med Sci Sports Exerc.*, *33*(8), 1361-1366.

Macdonald, J. H., Farina, D., & Marcora, S. M. (2008). Response of electromyographic variables during incremental and fatiguing cycling. *Med Sci Sports Exerc.*, *40*(2), 335-344.

Martin, J. C., & Brown, N. A. T. (2009). Joint-specific power production and fatigue during maximal cycling. *J Biomech.*, *42*(4), 474-479.

Mornieux, G., Zameziati, K., Rouffet, D., Stapelfeldt, B., Gollhofer, A., & Belli, A. (2006). Influence of pedalling effectiveness on the inter-individual variations of muscular efficiency in cycling. *Isokinet Exerc Sci.*, 14(1), 63-70.

Mujika, I., & Padilla, S. (2001). Physiological and performance characteristics of male professional road cyclists. *Sports Med.*, *31*(7), 479–487.

Neptune, R. R., Kautz, S. A., & Hull, M. L. (1997). The effect of pedaling rate on coordination in cycling. *J Biomech.*, *30*(10), 1051–1058.

Neptune, R. R., Kautz, S. A., & Zajac, F. E. (2000). Muscle contributions to specifc biomechanical functions do not change in forward versus backward pedaling. *J Biomech.*, *33*(2), 155–164.

Padilla, S., Mujika, I., Orbañanos, J., Santisteban, J., Angulo, F., & José Goiriena, J. (2001). Exercise intensity and load during mass-start stage races in professional road cycling. *Med Sci Sports Exerc.*, *33*(5), 796-802.

Patterson, R. P., & Moreno, M. I. (1990). Bicycle pedalling forces as a function of pedalling rate and power output. *Med Sci Sports Exerc.*, *22*(4), 512-516.

Patterson, R. P., Pearson, J. L., & Fisher, S. V. (1983). The influence of flywheel weight and pedalling frequency on the biomechanics and physiological responses to bicycle exercise. *Ergonomics.*, *26*(7), 659–668.

Petrofsky, J. S. (1979). Frequency and amplitude analysis of the EMG during exercise on the bicycle ergometer. *Eur J Appl Physiol.*, *41*(1), 1–15.

Rossato, M., Bini, R. R., Carpes, F. P., Diefenthaeler, F., & Moro, A. R. P. (2008). Cadence and workload effects on pedaling technique of well-trained cyclists. *Int J Sports Med.*, *29*(9), 746–752.

Ryan, M. M., & Gregor, R. J. (1992). EMG profiles of lower extremity muscles during cycling at constant workload and cadence. *J Electromyogr Kinesiol.*, *2*(2), 69–80.

Sanderson, D. J., & Black, A. (2003). The effect of prolonged cycling on pedal forces. *J Sports Sci.*, *21*(3), 191–199.

Sanderson, D. J. (1991). The influence of cadence and power output on the biomechanics of force application during steady-rate cycling in competitive and recreational cyclists. *J Sports Sci.*, *9*(2), 191-203.

Sarre, G., & Lepers, R. (2005). Neuromuscular function during prolonged pedalling exercise at different cadences. *Acta Physiol Scand.*, *185*(4), 321–328.

St Clair Gibson, A., Schabort, E. J., & Noakes, T. D. (2001). Reduced neuromuscular activity and force generation during prolonged cycling. *Am J Physiol-Reg I.*, *281*(1), 187–196.

Takaishi, T., Yasuda, Y., Ono, T., & Moritani, T. (1996). Optimal pedaling rate estimated from neuromuscular fatigue for cyclists. *Med Sci Sports Exerc.*, *28*(12), 1492-1497.

Tatterson, A. J., Hahn, A. G., Martini, D. T., & Febbraio, M. A. (2000). Effects of heat stress on physiological responses and exercise performance in elite cyclists. *J Sci Med Sport.*, *3*(2), 186–193.

van Ingen Schenau, G. J., Boots, P. J. M., de Groot, G., Snackers, R. J., & van Woensel, W. W. L. M. (1992). The constrained control of force and position in multi-joint movements. *Neuroscience*, *46*(1), 197-207.

Vogt, S., Heinrich, L., Schumacher, Y. O., Blum, A., Roecker, K., Dickhuth, H. H., & Schmid, A. (2006). Power output during stage racing in professional road cycling. *Med Sci Sports Exerc.*, *38*(1), 147-151.

von Tscharner, V. (2000). Intensity analysis in time-frequency space of surface myoelectric signals by wavelets of specified resolution. *J Electromyogr Kinesiol.*, *10*(6), 433-445.

Wakeling, J. M., Blake, O. M., & Chan, H. K. (2010). Muscle coordination is key to the power output and mechanical efficiency of limb movements. *J Exp Biol.*, *213*(3), 487-492.

Wakeling, J. M., Blake, O. M., Wong, I., Rana, M., & Lee, S. S. M. (2011). Movement mechanics as a determinate of muscle structure, recruitment and coordination. *Phil Trans R Soc B.*, *366*(1570), 1554-1564.

Wakeling, J. M., & Horn, T. (2009). Neuromechanics of muscle synergies during cycling. *J Neurophysiol.*, *101*(2), 843-854.

Wakeling, J. M., Pascual, S. A., Nigg, B. M., & Tscharner, V. (2001). Surface EMG shows distinct populations of muscle activity when measured during sustained sub-maximal exercise. *Eur J Appl Physiol.*, *86*(1), 40–47.

Whipp, B. J., & Wasserman, K. (1969). Efficiency of muscular work. *J Appl Physiol.*, *26*(5), 644–648.

Zameziati, K., Mornieux, G., Rouffet, D., & Belli, A. (2005). Relationship between the increase of effectiveness indexes and the increase of muscular efficiency with cycling power. *Eur J Appl Physiol.*, *96*(3), 274–281.